



**AFRL-RH-WP-SR-2016-0002**

**EFFECTS OF VARIABLE HELMET WEIGHT ON  
HUMAN RESPONSE TO  $-G_x$  IMPACT**

**John R. Buhrman, Grant C. Roush,  
Erica M. Johnson, Chris E. Perry**

**Warfighter Interface Division  
Applied Neuroscience Branch**

**Nathaniel R. Bridges, Stephen E. Mosher**

**Infocitex Corporation  
Technical Service Division  
4027 Colonel Glenn Highway, Suite 210  
Dayton OH 45431**

**Rachael A. Christopher  
Oakridge Institute for Science and Education  
Oak Ridge TN 37821**

**February 2016  
Interim Report**

**Distribution A: Approved for public release.**

*See additional restrictions described on inside pages*

**STINFO COPY**

**AIR FORCE RESEARCH LABORATORY  
711<sup>TH</sup> HUMAN PERFORMANCE WING,  
HUMAN EFFECTIVENESS DIRECTORATE,  
WRIGHT-PATTERSON AIR FORCE BASE, OH 45433  
AIR FORCE MATERIEL COMMAND  
UNITED STATES AIR FORCE**

## NOTICE AND SIGNATURE PAGE

Using Government drawings, specifications, or other data included in this document for any purpose other than Government procurement does not in any way obligate the U.S. Government. The fact that the Government formulated or supplied the drawings, specifications, or other data does not license the holder or any other person or corporation; or convey any rights or permission to manufacture, use, or sell any patented invention that may relate to them.

This report was cleared for public release by the 88<sup>th</sup> Air Base Wing Public Affairs Office and is available to the general public, including foreign nationals. Copies may be obtained from the Defense Technical Information Center (DTIC) (<http://www.dtic.mil>).

AFRL-RH-WP-SR-2016-0002 HAS BEEN REVIEWED AND IS APPROVED FOR PUBLICATION IN ACCORDANCE WITH ASSIGNED DISTRIBUTION STATEMENT.

//signed//

CHRIS M. BURNEKA  
Work Unit Manager  
Applied Neuroscience Branch

//signed//

SCOTT M. GALSTER  
Chief, Applied Neuroscience Branch  
Warfighter Interface Division

//signed//

WILLIAM E. RUSSELL  
Chief, Warfighter Interface Division  
Human Effectiveness Directorate

This report is published in the interest of scientific and technical information exchange, and its publication does not constitute the Government's approval or disapproval of its ideas or findings.

<b>REPORT DOCUMENTATION PAGE</b>			<i>Form Approved</i> <i>OMB No. 0704-0188</i>		
Public reporting burden for this collection of information is estimated to average 1 hour per response, including the time for reviewing instructions, searching existing data sources, gathering and maintaining the data needed, and completing and reviewing this collection of information. Send comments regarding this burden estimate or any other aspect of this collection of information, including suggestions for reducing this burden to Department of Defense, Washington Headquarters Services, Directorate for Information Operations and Reports (0704-0188), 1215 Jefferson Davis Highway, Suite 1204, Arlington, VA 22202-4302. Respondents should be aware that notwithstanding any other provision of law, no person shall be subject to any penalty for failing to comply with a collection of information if it does not display a currently valid OMB control number. <b>PLEASE DO NOT RETURN YOUR FORM TO THE ABOVE ADDRESS.</b>					
<b>1. REPORT DATE (DD-MM-YYYY)</b> 26-02-2016		<b>2. REPORT TYPE</b> Interim Report		<b>3. DATES COVERED (From - To)</b> Feb 2003 – Feb 2016	
<b>4. TITLE AND SUBTITLE</b>  Effects of Variable Helmet Weight on Human Response to –Gx Impact			<b>5a. CONTRACT NUMBER</b> In-House		
			<b>5b. GRANT NUMBER</b>		
			<b>5c. PROGRAM ELEMENT NUMBER</b> 62202F		
<b>6. AUTHOR(S)</b> *John R. Buhrman      **Nathanial R. Bridges      ***Rachael A. Christopher Grant C. Roush              Steven E. Mosher Erica M. Johnson Chris E. Perry			<b>5d. PROJECT NUMBER</b>		
			<b>5e. TASK NUMBER</b>		
			<b>5f. WORK UNIT NUMBER</b> HOEE (53290811)		
<b>7. PERFORMING ORGANIZATION NAME(S) AND ADDRESS(ES)</b> **Infoscitex Corporation                      ***ORISE Technical Service Division                      1299 Bethel Valley Road 4027 Colonel Glenn Highway, Suite 210      Oak Ridge TN 37831 Dayton OH 45431			<b>8. PERFORMING ORGANIZATION REPORT NUMBER</b>		
<b>9. SPONSORING / MONITORING AGENCY NAME(S) AND ADDRESS(ES)</b> *Air Force Materiel Command Air Force Research Laboratory 711 Human Performance Wing Human Effectiveness Directorate Warfighter Interface Division Applied Neuroscience Branch Wright-Patterson AFB OH 45433			<b>10. SPONSOR/MONITOR'S ACRONYM(S)</b> 711 HPW/RHCP		
			<b>11. SPONSOR/MONITOR'S REPORT NUMBER(S)</b> AFRL-RH-WP-SR-2016-0002		
<b>12. DISTRIBUTION / AVAILABILITY STATEMENT</b> Distribution A: Approved for public release.					
<b>13. SUPPLEMENTARY NOTES</b> 88ABW Cleared 04/25/2016; 88ABW-2016-2080.					
<b>14. ABSTRACT</b> Helmet-mounted systems (HMS) may increase the potential for aircrew neck injury during aircraft ejection due to the increase in dynamic loads generated in the cervical spine as a result of the change in helmet inertial properties. A series of tests were conducted on a horizontal impulse accelerator with human subjects wearing forward-weighted helmets to investigate the effects of helmet inertial properties and bracing on human response to short-duration frontal (-Gx) impacts, as might be experienced during the seat deceleration and parachute opening shock phases of ejection. The tests demonstrated that some subjects began experiencing discomfort and pain when wearing 3.5 lb helmets at 10 G seat accelerations. While overall neck loads demonstrated little or no gender difference, the female subjects were on average unable to sustain as forceful a brace during pre-impact as the males, which may account for their higher head accelerations and higher percentage of reported adverse effects. Pilot bracing techniques may therefore have a beneficial effect on injury risk by off-loading some of the neck loads experienced during ejection.					
<b>15. SUBJECT TERMS</b> Frontal Impact, Impact Acceleration, Horizontal Impulse Accelerator, Helmet Mounted Systems, Helmet Weight, Ejection Injury, Pilot Bracing, Gender Acceleration Effects					
<b>16. SECURITY CLASSIFICATION OF:</b>			<b>17. LIMITATION OF ABSTRACT</b>	<b>18. NUMBER OF PAGES</b>	<b>19a. NAME OF RESPONSIBLE PERSON</b>
<b>a. REPORT</b>	<b>b. ABSTRACT</b>	<b>c. THIS PAGE</b>			Chris M. Burneka
Unclassified	Unclassified	Unclassified	SAR	86	<b>19b. TELEPHONE NUMBER (include area code)</b>

## TABLE OF CONTENTS

LIST OF FIGURES .....	iii
LIST OF TABLES .....	iv
PREFACE .....	v
1.0 INTRODUCTION .....	1
2.0 BACKGROUND .....	2
3.0 METHODS .....	3
4.0 RESULTS .....	7
4.1 Acceleration Response.....	7
4.2 Neck Loads .....	10
4.3 Neck Moments .....	12
4.4 Pre-Impact Headrest Bracing Loads .....	14
4.5 Effects of Subject Bracing .....	15
4.6 Head Displacements.....	17
4.7 Discomfort Incidences (Subjective).....	18
5.0 DISCUSSION .....	21
6.0 CONCLUSIONS.....	24
7.0 REFERENCES .....	25
APPENDIX A: Summary Statistical Data Sheet .....	26
APPENDIX B: Test Configuration and Data Acquisition System .....	29
APPENDIX C: Subject Anthropometry Data.....	50
APPENDIX D: Electronic Data Channels .....	52
APPENDIX E: Weight and Center-of-Gravity of Helmet Configurations.....	55
APPENDIX F: Neck Load Program .....	57
APPENDIX G: Sample Acceleration/Force Data.....	62

**LIST OF FIGURES**

Figure 1. Horizontal Impulse Accelerator (HIA) ..... 3

Figure 2. Side View of the Test Setup with Subject in the Initial Position ..... 4

Figure 3. Modified HGU-55/P Flight Helmet for Weight Attachment along a Halo on Each Side ..... 5

Figure 4. Anatomical Axis System of the Human Head ..... 6

Figure 5. Head X-Axis Acceleration Response Summary as a Function of Helmet Weight (8 G) ..... 8

Figure 6. Head X-Axis Acceleration Response Summary as a Function of Sled Acceleration (4.5 lb Helmet) ..... 9

Figure 7. Head X-Axis Acceleration Response Summary as a Function of Sled Acceleration (3.0 lb Helmet) ..... 9

Figure 8. Gender Comparison of X-Axis Neck Loads as a Function of Helmet Weight (8 G) .. 10

Figure 9. Neck X-Axis Loads as a Function of Sled Acceleration Level (4.5 lb Helmet) ..... 11

Figure 10. Neck X-Axis Load as a Function of Sled Acceleration Level (3.0 lb Helmet) ..... 12

Figure 11. Gender Comparison of Neck Moments ( $M_y$ ) as a Function of Helmet Weight ..... 13

Figure 12. Neck  $M_y$  Moments as a Function of Sled Acceleration Level (4.5 lb Helmet) ..... 13

Figure 13. Neck  $M_y$  Moments as a Function of Sled Acceleration Level (3.0 lb Helmet) ..... 14

Figure 14. Pre-impact Headrest Load with Increasing Helmet Weight (at 8G) ..... 15

Figure 15. Bracing Effects on Head X-Axis Acceleration at 8 G with 3.0 lb Helmet ..... 16

Figure 16. Bracing Effects on Neck X-Axis Load at 8 G with 3.0 lb Helmet ..... 17

Figure 17. Bracing Effects on Neck Moments ( $M_y$ ) at 8 G with 3.0 lb Helmet ..... 17

Figure 18. Gender Comparison of Peak Resultant Displacement as a Function of Helmet Weight (at 8 G) ..... 18

## LIST OF TABLES

Table 1. Variable Weighted Impact (VWI) Helmet Test Matrix .....	4
Table 2. Summary of Subject Anthropometry Averages .....	5
Table 3. General Mean Peak X-Axis Acceleration Summary (all conditions) .....	7
Table 4. Head X-Axis Acceleration Response Summary (8 G) .....	8
Table 5. Head X-Axis Acceleration Response Summary (4.5 lb Helmet) .....	8
Table 6. Head X-Axis Acceleration Response Summary (3.0 lb Helmet) .....	9
Table 7. Gender Specific Peak Neck X-Axis Loads (at 8 G) .....	10
Table 8. Gender Specific Peak Neck X-Axis Loads (4.5 lb Helmet) .....	11
Table 9. Gender Specific Peak Neck X-Axis Loads (3.0 lb Helmet) .....	11
Table 10. Gender Specific Peak Neck $M_y$ Moment Responses (at 8 G) .....	12
Table 11. Gender Specific Peak Neck $M_y$ Moment Responses (4.5 lb helmet) .....	13
Table 12. Gender Specific Peak Neck $M_y$ Moment Responses (3.0 lb helmet) .....	14
Table 13. Headrest Bracing Loads for 8 G Sled Accelerations .....	15
Table 14. Mean and SD of all Headrest Bracing Loads .....	15
Table 15. Comparison of Headrest Loads in Moderate and Full Bracing Tests .....	16
Table 16. Gender Comparison of Resultant Displacements at Mouth .....	18
Table 17. Discomfort Incidences with Respect to Gender (Neck and Back) .....	19
Table 18. Discomfort Incidences with Respect to Gender, Helmet Weight, and Sled Acceleration (Neck and Back – Includes General Symptoms) .....	20

## **PREFACE**

The impact tests and data analysis described in this report were accomplished by the Applied Neuroscience Branch of the Warfighter Interface Division (formerly the Vulnerability Analysis Branch of the Biosciences and Protection Division), Human Effectiveness Directorate of the Air Force Research Laboratory (711 HPW/RHCP) at Wright-Patterson Air Force Base, Ohio. The test facility for this study was the Horizontal Impulse Accelerator (HIA). Engineering support was provided by General Dynamics AIS under contract F41624-97-D-6004 and Infoscitex under FA8650-09-D-6949.

## 1.0 INTRODUCTION

Helmet-mounted systems (HMS), such as night vision goggles and helmet-mounted displays, are designed to enhance pilot performance through improvement in situational awareness, target acquisition and weapon delivery. Using HMS, however, may also affect pilot safety by increasing the potential for neck injury during all phases of ejection (catapult stroke, windblast, seat stabilization, and parachute opening shock). This increased neck injury potential is due to the increase in dynamic loads generated in the cervical spine as a result of the change in helmet inertial properties including weight, center-of-gravity (CG), and moments-of-inertia (MOI). Pilot bracing techniques may also have an effect on ejection injury risk by off-loading some of the neck loads during impact acceleration. Research is therefore required to establish the relationship between helmet inertial properties and human impact response in the three coordinate axes. Test results can then be used to define acceptable helmet inertial properties for the ejection environment and to improve bracing techniques to minimize pilot injury during ejection.

A series of tests were conducted to investigate the effects of helmet inertial properties and bracing on human response to short-duration frontal (-Gx) impacts of variable magnitude. Tests were conducted at peak acceleration levels from 6 to 10 G, with pulse duration of approximately 150 ms. Total head supported weight varied from 0 (no helmet) to 4.5 lbs.

## **2.0 BACKGROUND**

The Air Force Research Laboratory has been extensively involved over the past two decades in conducting dynamic human impact testing in different axes to investigate the effect on human response and injury risk of helmet inertial properties. Test programs conducted by Perry, Buhrman, and associates [1,6,7,8,10] at the Air Force Research Laboratory's former Biomechanics Branch (711 HPW/RHPA) from 1989 through 2001 evaluated the effects of variable helmet inertial properties on the biodynamic response of male and female human volunteers exposed to vertical (+Gz) accelerations with helmet weights up to 7 lbs using the Vertical Deceleration Tower (VDT). A 2003 study by Perry and Buhrman [9] investigated the effects of varied helmet weight up to 4.5 lbs on human response during lateral (+Gy) impact accelerations on the Horizontal Impulse Accelerator (HIA). A 2003 study by Pint [11] explored the effects of varied helmet weight up to 5 lbs on human neck response during retraction, similar to that experienced by aircrew during the pre-ejection "haulback" phase, using the AFRL Body Positioning and Restraint Device (BPRD).

Additional dynamic response data from a -Gx impact environment with variable helmet weight are required to continue the development of a human biodynamic response database for the three coordinate axes, and to continue the development of human biodynamic response models and multi-axial neck injury criteria. The objective of this study was to provide these additional human dynamic response data and an analysis of the effects of varying helmet properties. The results of this program will contribute to the development of design guidelines for the safe use of helmet-weighted systems and provide information on optimal pilot bracing techniques.

### 3.0 METHODS

A series of short-duration frontal impact tests were conducted with male and female volunteer subjects using the AFRL Horizontal Impulse Accelerator (HIA) located at Wright-Patterson AFB, OH. The HIA (also referred to as the ‘sled track’) consists of a 4’ x 8’ sled positioned on a 204 ft. long track, and is accelerated using a 24-inch diameter pneumatic actuator (Figure 1). The HIA operates on the principle of differential gas pressures acting on both surfaces of a thrust piston in a closed cylinder. The impact acceleration occurs at the beginning of the experiment as stored high-pressure air is allowed to impinge on the surface of the thrust piston thus propelling the sled. As the sled breaks contact with the thrust piston, the sled coasts to a stop, or is stopped with a triggered pneumatic brake system.

The frontal acceleration profile generated by the HIA approximated a half-sine pulse with rise-time of approximately 75 ms and pulse duration of 150 ms. The peak of the impact pulse varied in magnitude from 6 to 10 G, and head supported helmet weights ranged from 0.0 lbs (no helmet) to 4.5 lbs (Table 1). The acceleration levels had been previously tested, and were well tolerated by volunteer human subjects while wearing a standard HGU-55/P helmet with no added weight [2]. Prior to human testing, tests were conducted in each condition with an instrumented Large Advanced Dynamic Anthropomorphic Manikin (ADAM) to ensure that the test conditions were within safe limits.

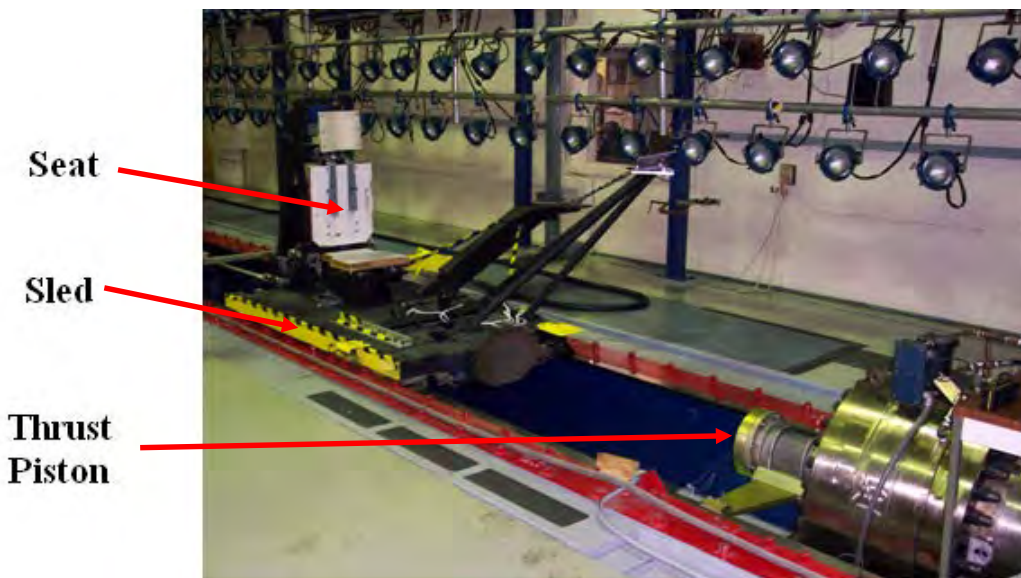


**Figure 1. Horizontal Impulse Accelerator (HIA)**

**Table 1. Variable Weighted Impact (VWI) Helmet Test Matrix**

G Level	Helmet Weight (lb)					
	0.0 (no helmet)	2.0	3.0	3.5	4.0	4.5
6			J1/T2		A2	C/C1
7						W/W1
8			L/L1, LR/LR1*	V/V1	B	D/D1
10	E/E1	X/X1	F/F1	M		

\*Cell LR required the subjects to brace at less than their maximum, approximating 20 lbs of load on the headrest

All tests were conducted using the generic “40G Seat” mounted on the HIA sled. The seat was mounted such that the input acceleration pulse was applied into the chest of the subject (frontal impact). All subjects (human and manikin) were seated in an upright position and restrained to the seat (Figure 2). A contoured headrest was used for all cells which was in-line with the seat back. The seat back was perpendicular to the seat pan, and the seat pan was parallel to the horizontal plane of the sled. All subjects were fitted with a PCU-15/P or 16/P harness prior to being positioned in the seat. Each subject also wore a standard HBU lap belt. The restraint straps were pre-tensioned at the shoulder and the lap attachment points to  $20 \pm 5$  lbs prior to each test. The subjects’ feet were individually restrained using Velcro straps attached to the footrests mounted on the floor of the sled. The subjects’ hands were positioned to grip the Velcro thigh straps with palms facing down.



**Figure 2. Side View of the Test Setup with Subject in the Initial Position**

The subject population consisted of the large manikin (ADAM) and thirty-four human subjects; sixteen females and eighteen males. All human subjects were members of the 711 HPW/RH Impact Acceleration Test Panel. Each subject completed a series of individual anthropometric measurements (Appendix C). The subjects ranged in age, weight, and height as shown in Table 2. This test program was formally approved by the Wright Research Site Institutional Review Board (WRS IRB) under protocol F-WR-2003-0014-H.

**Table 2. Summary of Subject Anthropometry Averages**

Gender	Age (yr)	Weight ( lbs)	Standing Ht. (in)	Sitting Ht. (in)
Males	30.1 ± 4.9	187.8 ± 35.2	70.8 ± 2.0	37.0 ± 1.2
Females	26.7 ± 6.3	147.2 ± 20.4	64.6 ± 3.2	34.2 ± 1.2

As seen in Table 1, the total head supported weight ranged from 0.0 (no helmet) to 4.5 lbs. The helmets used were a standard lightweight HGU-55/P and a variable weighted impact (VWI) or ‘Halo’ helmet. The VWI is an HGU-55/P helmet that was modified for weight attachment at various center-of-gravity locations (Figure 3), and is used to simulate the mass properties of current Air Force front-loaded helmet-mounted systems. Subjects were fitted with a medium, large, or extra-large size helmet for both the standard HGU-55/P and VWI configurations weighing between 2.0 and 4.5 lbs with forward center-of-gravity (Appendix E).



**Figure 3. Modified HGU-55/P Flight Helmet for Weight Attachment along a Halo on Each Side**

Measured electronic data collected during each test included sled velocity and accelerations, seat accelerations, subject head and chest accelerations and displacements, and loads developed in the seat and the restraint system. Data are presented in the anatomical axis system referenced below (Figure 4). Tri-axial accelerometer packages were used to record seat pan and sled accelerations. Load cells were used to measure the loads generated at the seat pan, headrest, and lap and shoulder strap attachment points. The head accelerations were measured with a tri-axial accelerometer array mounted on a bite bar. The bite bar accelerometer array also contained an angular accelerometer to record rotational acceleration about the y-axis (positive Y moment represents forward flexion). A linear X accelerometer and angular Y rate sensor were placed on the chest using an adhesive Velcro strap. Tri-axial earplug accelerometers were mounted in both ears for some tests (designated with a “1”, e.g. E1). Head displacement data were collected using two Weinberger high speed video cameras that recorded the position of 10 displacement markers at 500 samples per second. Processed motion analysis data consisted of relative displacement curves, and displacement and velocity time histories for the six subject mounted markers. For details on the instrumentation, refer to Appendix B.

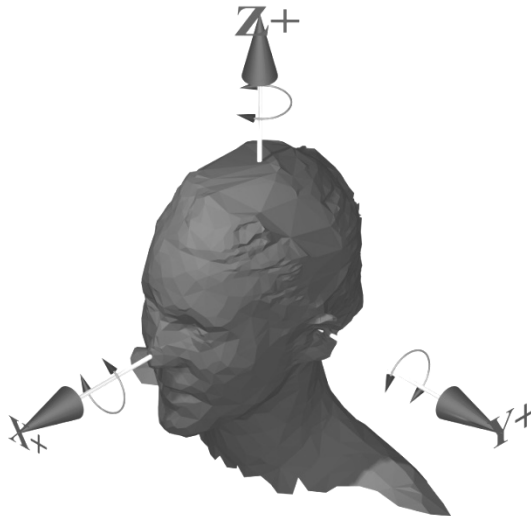


**Figure 4. Anatomical Axis System of the Human Head**

All test data were organized in individual test data files containing channel time histories, peak and time-to-peak analysis, and summary plots. In the peak value analysis, a time frame of 200 ms was used to omit from the evaluation any acceleration peaks due to headrest strikes following head rebound. Each test cell had its corresponding data organized into a file containing simple summary statistics (mean and standard deviation) on the measured and calculated parameters. One test cell file was designated for the maximum values and one file for the minimum values. The statistical analyses were performed on the data using Microsoft® Excel 2002/2007/2010 and SAS version 9.2, which are both commercially available software packages. With this software, parameters such as confidence intervals and p-values were used to compare and draw statistical significances from the data.

The human subjects' neck loads and moments, generated at the occipital condyle (OC, or head-neck joint), were calculated using measured head acceleration and inertial property data. An in-house program, "Neckload4," used the head acceleration time histories (collected with the bite bar instrumentation package) and the inertial properties of the head/helmet to approximate the load and moment time histories at the occipital condyle, as described in Appendix F and [3]. The inertial properties were calculated by a sub-routine of "Neckload4" called "Combine." "Combine" approximates the inertial properties of the subject's head with helmet using the subject's total body weight, head circumference, and previously measured helmet inertial properties. Because "Neckload4" does not take into account external loads on the head, the program output represents the loads and moments after the head has separated from the headrest. MATLAB®2011 was then used to extract and compile the maximum neck load and neck moment values for statistical analysis.

The measured headrest pre-impact loads were statistically evaluated for all of the test runs. The headrest pre-impact load is the magnitude of load applied to the headrest by the subject just prior to impact as a result of required bracing techniques. The subjects were instructed to perform a maximum brace just prior to impact which averaged between 35-50 lbs of force against the headrest, although some subjects braced at higher and lower levels. A real-time headrest load monitor was used so that subjects could adjust their brace accordingly. For cell LR, the subjects were instructed to brace at a lower level of  $20 \pm 5$  lbs of headrest load.

## 4.0 RESULTS

The following tables highlight the findings for subject acceleration responses, neck loads, neck moments, pre-impact bracing loads, head displacements as well as test discomfort indices. For a summary of all the numerical data and cells used in the study, additional statistical values, a listing of the outliers removed from specific cells, and number of remaining subjects in each cell, see Appendix A.

### 4.1 Acceleration Response

Test runs that were greater than 2.5 standard deviations from the mean were identified and removed from the data set if considered outliers (see Appendix A). On occasion, subjects also repeated cell conditions if the test conductor indicated an error with the run. Since these test runs were duplicates of the same condition only the later trial was used in the analysis. The sled, seat, chest, and head acceleration responses in the direction of impact are summarized in Table 3. The combined (male and female) mean and standard deviation are identified for each parameter in each of the selected test conditions. The small standard deviation values of the sled acceleration indicate excellent control of the sled parameters. The mean peak values of the seat acceleration were slightly higher than the mean sled acceleration due to small vibrations in the seat. Chest peak acceleration values tended to be higher than seat acceleration values, while peak head acceleration values were the highest. On average, the input acceleration was amplified by a factor of 1.3 at the head of the human subjects (compared to peak sled acceleration). This amplification factor increased slightly (from 1.2 to 1.4) as sled acceleration increased.

**Table 3. General Mean Peak X-Axis Acceleration Summary (all conditions)**

Nominal Sled Accel (G)	Sled X Accel (G)	Seat X Accel (G)	Chest X Accel (G)	Head X Accel (G)
<b>6 (J1, T2, A2, C)</b>	6.01 ± 0.11	6.07 ± 0.10	6.27 ± 1.08	7.13 ± 1.23
<b>7 (W)</b>	7.12 ± 0.07	7.17 ± 0.10	6.99 ± 1.44	8.73 ± 1.18
<b>8 (L, V, B, D)</b>	7.94 ± 0.10	8.05 ± 0.10	8.40 ± 1.51	10.66 ± 1.74
<b>10 (E, X, F, M)</b>	9.99 ± 0.14	9.99 ± 0.15	10.78 ± 1.96	13.83 ± 2.54

T-tests were performed on the head accelerations in the x-axis (linear) direction (Tables 4-6). For females, as head supported weight was increased from 3.0 to 3.5 lbs, the linear head acceleration slightly increased (Table 4, Figure 5). However, at 4.0 lbs the average head acceleration decreased, increasing again when the helmet weight was increased to 4.5 lbs. For male subjects, average head accelerations slightly increased as helmet weight increased from 3.0 to 3.5 lbs and again from 3.5 to 4.0 lbs. Average head acceleration, however, decreased when helmet weight was increased from 4.0 to 4.5 lbs. (Table 4, Figure 5). For cases of increasing sled acceleration, a linear relationship was observed as head acceleration increased with sled acceleration for both male and female subjects (Tables 5 and 6, Figures 6 and 7). In general, females showed higher peak acceleration averages compared to males.

**Table 4. Head X-Axis Acceleration Response Summary (8 G)**

Helmet Weight (lbs)	Head X Accel, Males (G)	Head X Accel, Females (G)	Percent Difference	P
3.0 (L)	9.81 ± 1.59	11.00 ± 1.15	12.1%	0.04
3.5 (V)	10.11 ± 1.51	11.66 ± 1.69	15.3%	0.03
4.0 (B)	11.10 ± 2.32	10.80 ± 1.64	-2.7%	0.70
4.5 (D)	10.11 ± 1.71	10.99 ± 1.49	8.7%	0.22

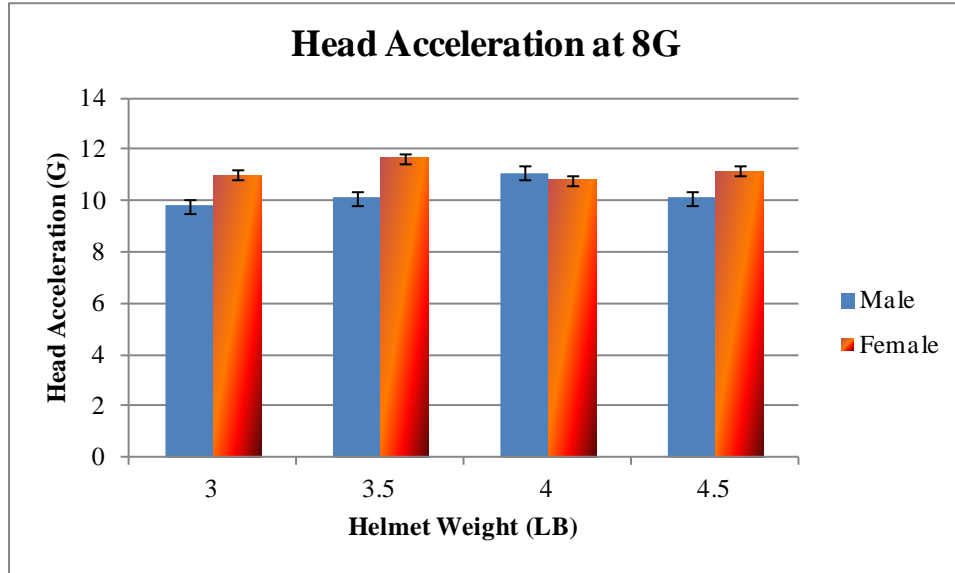


**Figure 5. Head X-Axis Acceleration Response Summary as a Function of Helmet Weight (8 G)**

For tests with the 4.5 lb helmet (Table 5 and Figure 6), females experienced greater average head acceleration than males in all cells. The largest difference of 19% occurred in the 7 G condition, which was the only cell showing a significant difference ( $\alpha = 0.05$ ).

**Table 5. Head X-Axis Acceleration Response Summary (4.5 lb Helmet)**

Sled Accel (G)	Head X Accel, Males (G)	Head X Accel, Females (G)	Percent Difference	P
6 (C)	6.75 ± 1.31	7.21 ± 0.77	6.8%	0.31
7 (W)	7.94 ± 0.66	9.45 ± 1.10	19.0%	0.00
8 (D)	10.11 ± 1.71	10.99 ± 1.49	8.7%	0.22

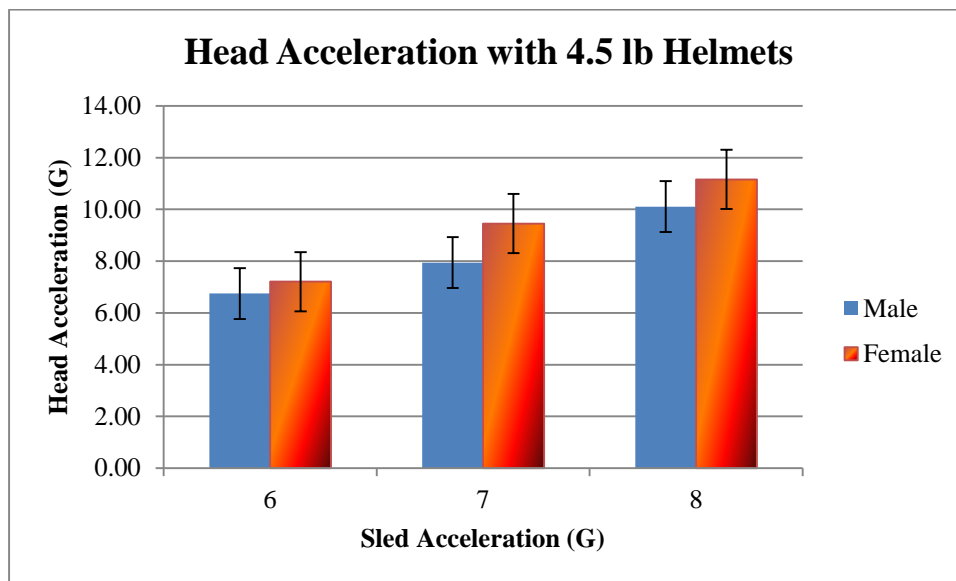


**Figure 6. Head X-Axis Acceleration Response Summary as a Function of Sled Acceleration (4.5 lb Helmet)**

For the 3.0 lb helmet weight (Table 6 and Figure 7), females demonstrated higher average peak head accelerations than males in all cells, which were significant in the 8 G condition ( $\alpha = 0.05$ ).

**Table 6. Head X-Axis Acceleration Response Summary (3.0 lb Helmet)**

Sled Accel (G)	Head X Accel, Males (G)	Head X Accel, Females (G)	Percent Difference	p
6 (J1/T2)	6.58 ± 0.59	7.38 ± 1.08	12.2%	0.06
8 (L)	9.81 ± 1.59	11.00 ± 1.15	12.1%	0.04
10 (F)	14.14 ± 2.84	14.80 ± 3.25	4.7%	0.73

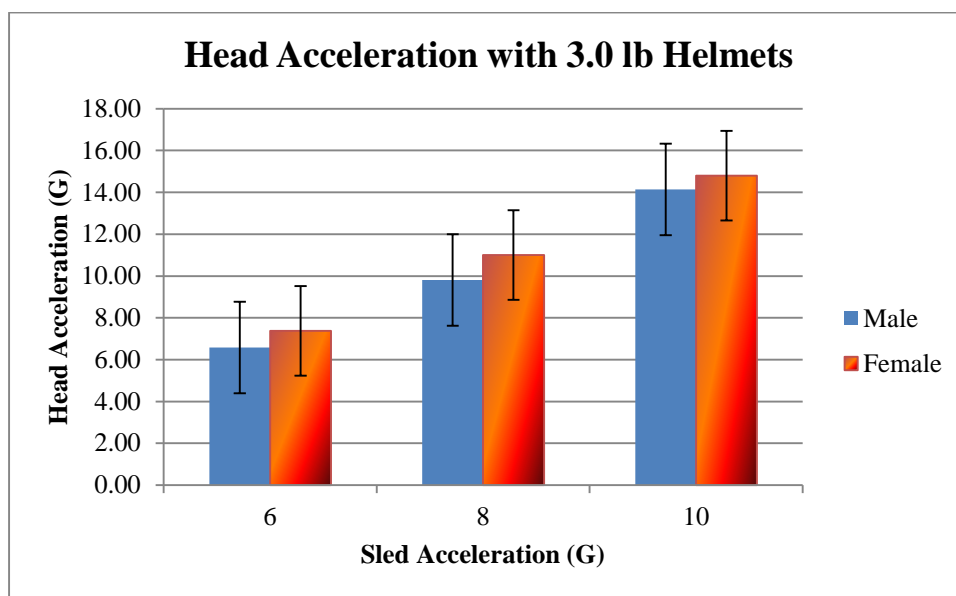


**Figure 7. Head X-Axis Acceleration Response Summary as a Function of Sled Acceleration (3.0 lb Helmet)**

## 4.2 Neck Loads

The following neck load data were calculated using the “Neckload4” program (Appendix F). As described in “Methods”, this program does not take into account the external loads on the head resulting from the headrest. The mean peak neck loads were calculated, averaged, and plotted against both increasing helmet weight and sled acceleration level.

At constant 8 G sled acceleration, males and females experienced similar neck loads for all helmet weights (Table 7 and Figure 8) which generally increased with increasing helmet weight. No statistical significances gender differences were present for any of the different helmet weight conditions ( $\alpha = 0.05$ ).

**Table 7. Gender Specific Peak Neck X-Axis Loads (at 8 G)**

Helmet Weight (lbs)	Neck Load, Males (lbs)	Neck Load, Female (lbs)	Percent Difference	p
<b>3.0 (L)</b>	111.92 ± 17.01	103.15 ± 12.93	-7.8%	0.16
<b>3.5 (V)</b>	119.09 ± 16.68	115.00 ± 17.46	-3.4%	0.56
<b>4.0 (B)</b>	130.32 ± 25.92	117.72 ± 18.66	-9.7%	0.15
<b>4.5 (D)</b>	130.17 ± 19.66	129.68 ± 23.03	-0.4%	0.96

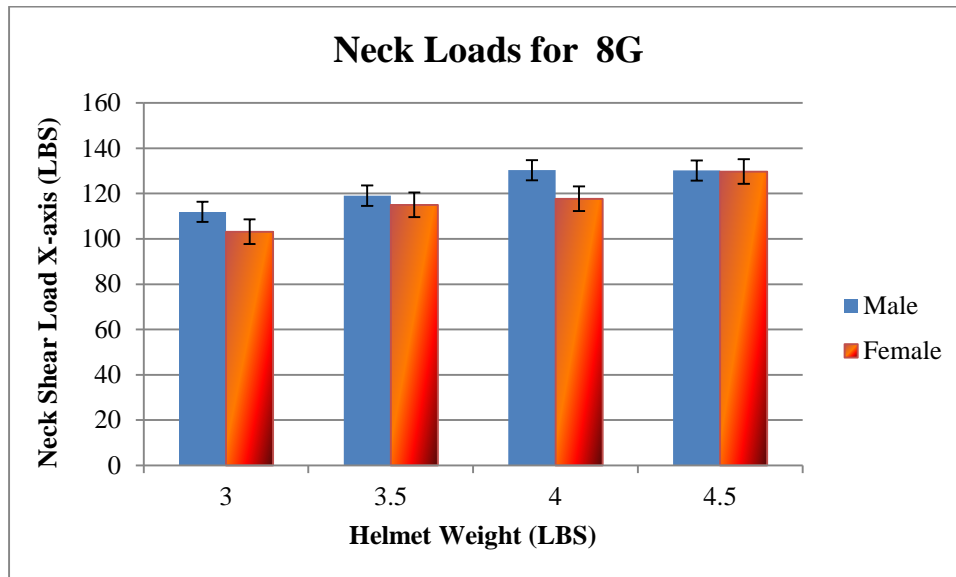


**Figure 8. Gender Comparison of X-Axis Neck Loads as a Function of Helmet Weight (8 G)**

The shear neck loads (X) increased for both males and females with increasing sled acceleration level and constant 4.5 lb helmet weight (Table 8 and Figure 9). No statistically significant differences existed between male and female neck loads for sled accelerations of 6 G, 7 G and 8 G while wearing 4.5 lb helmets.

**Table 8. Gender Specific Peak Neck X-Axis Loads (4.5 lb Helmet)**

Sled Acceleration (G)	Male Average (lbs)	Female Average (lbs)	Percent Difference	P
6 (C)	88.03 ± 16.06	86.11 ± 13.19	-2.2%	0.75
7 (W)	106.90 ± 15.38	115.21 ± 23.17	7.8%	0.35
8 (D)	130.17 ± 19.66	129.68 ± 23.03	-0.4%	0.96

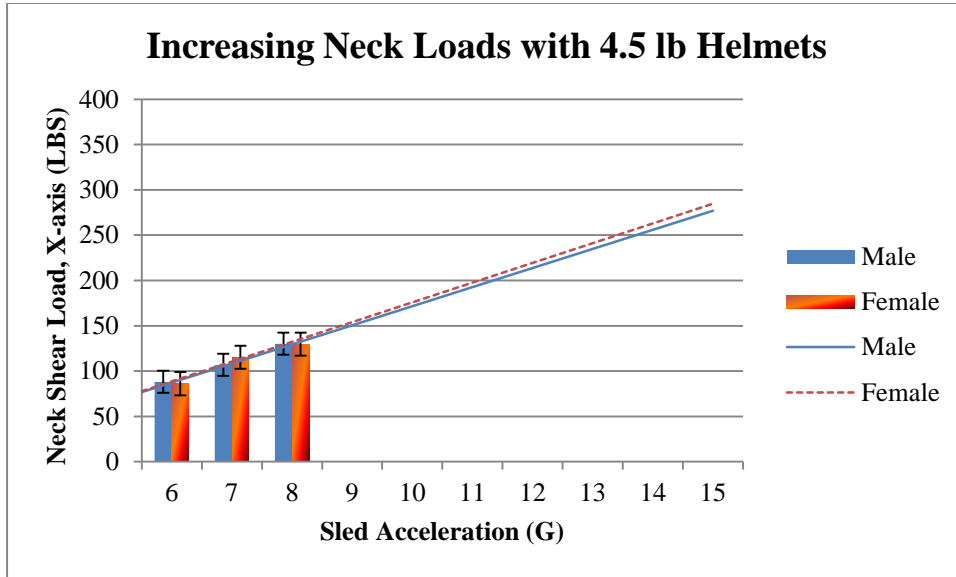


**Figure 9. Neck X-Axis Loads as a Function of Sled Acceleration Level (4.5 lb Helmet)**

Peak neck loads for both males and females during 3.0 lb helmet tests increased with increasing sled acceleration level (Table 9 and Figure 10). Neck loads were consistently higher for males, showing significant difference in the 6 G condition ( $\alpha = 0.05$ ).

**Table 9. Gender Specific Peak Neck X-Axis Loads (3.0 lb Helmet)**

Sled Accel (G)	Male Average (lbs)	Female Average (lbs)	Percent Difference	P
6 G (T2)	81.11 ± 9.58	71.84 ± 7.70	-11.4%	0.01
8 G (L)	111.92 ± 17.01	103.15 ± 12.93	-7.8%	0.16
10 G (F)	160.66 ± 44.82	157.36 ± 48.07	-2.1%	0.91

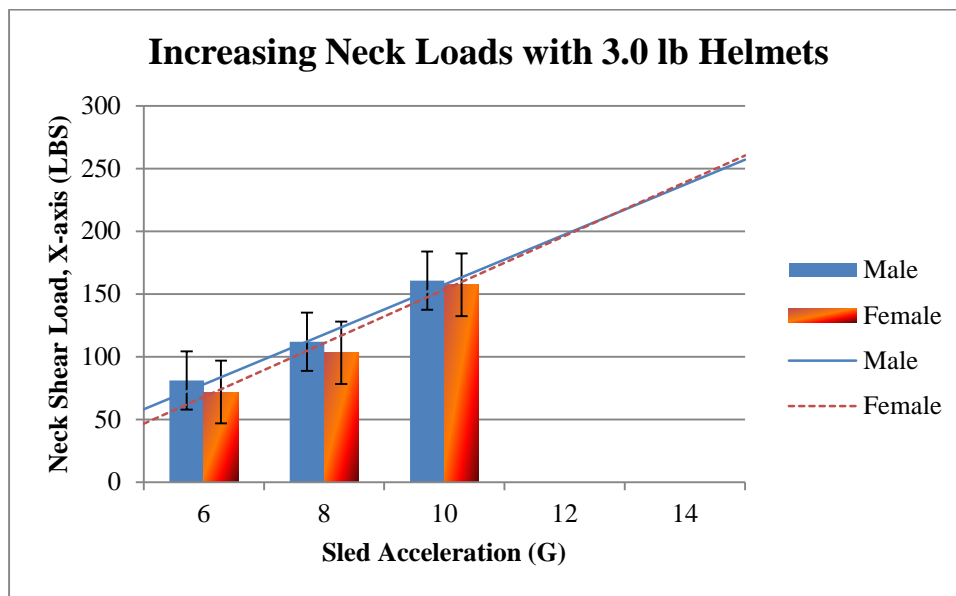


Figure 10. Neck X-Axis Load as a Function of Sled Acceleration Level (3.0 lb Helmet)

### 4.3 Neck Moments

Male and female Neck Y Moments (pitch) for varying helmet weights are recorded in Table 10 (see also Figure 11) for a constant 8 G sled acceleration. In general, the moments tended to increase slightly with increasing helmet weight for both males and females, although this trend was not analyzed for significance. No significant differences were observed ( $\alpha = 0.05$ ) between males and females for any of the helmet weight conditions at this acceleration level, although the males in general demonstrated slightly greater moments.

Table 10. Gender Specific Peak Neck  $M_y$  Moment Responses (at 8 G)

Helmet Weight (lbs)	Male Average (in-lbs)	Female Average (in-lbs)	Percent Difference	p
3.0 (L)	357.63 ± 66.61	346.66 ± 72.04	-3.1%	0.69
3.5 (V)	379.58 ± 83.56	395.33 ± 94.50	4.1%	0.67
4.0 (B)	435.58 ± 121.43	408.29 ± 88.35	-6.3%	0.50
4.5 (D)	435.77 ± 93.13	396.56 ± 43.96	-9.0%	0.25

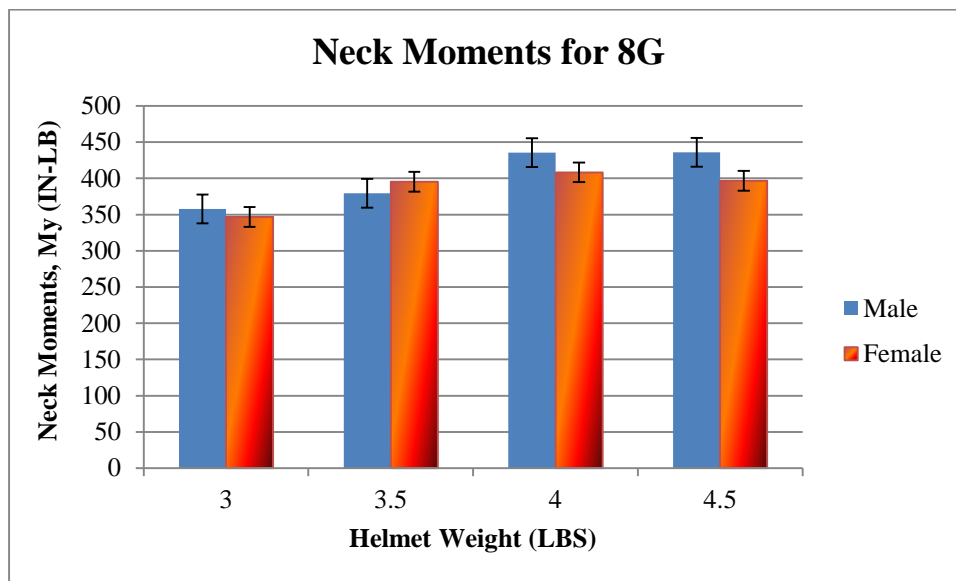


**Figure 11. Gender Comparison of Neck Moments ( $M_y$ ) as a Function of Helmet Weight**

When helmet weight was held constant at 4.5 lbs (Table 11 and Figure 12), no statistically significant differences were observed between genders at any of the acceleration conditions. In general, the moments increased for both males and females when moving from 6 to 8 G sled accelerations.

**Table 11. Gender Specific Peak Neck  $M_y$  Moment Responses (4.5 lb helmet)**

Sled Acceleration (G)	Male Average (in- lbs)	Female Average (in- lbs)	Percent Difference	P
6 (C)	325.93 ± 74.76	329.44 ± 66.96	1.1%	0.90
7 (W)	393.31 ± 93.77	397.43 ± 110.40	1.0%	0.93
8 (D)	435.77 ± 93.13	396.56 ± 43.96	-9.0%	0.25

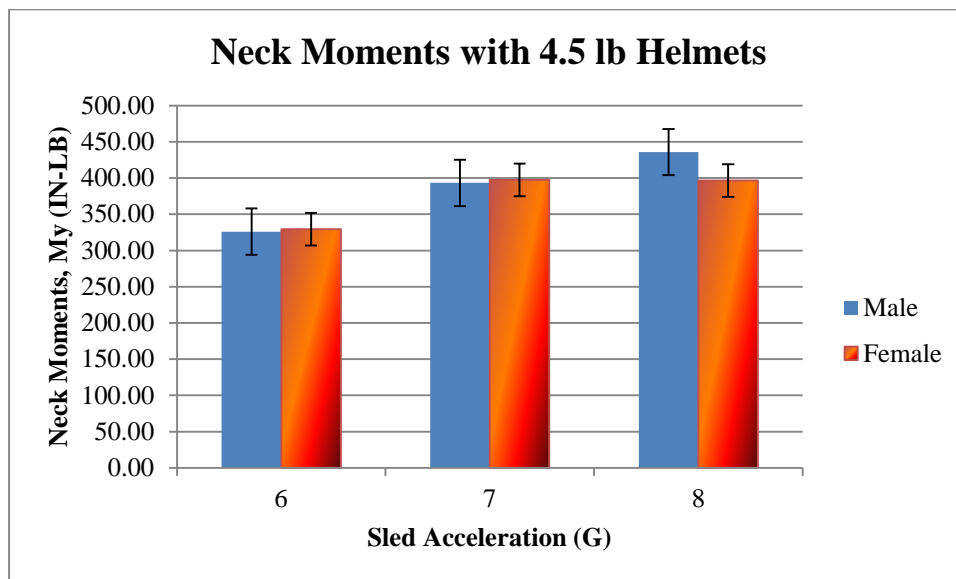


**Figure 12. Neck  $M_y$  Moments as a Function of Sled Acceleration Level (4.5 lb Helmet)**

Average neck moments ( $M_y$ ) were similar for males and females at various sled acceleration levels when a 3.0 lb helmet was worn (Table 12 and Figure 13), with no significant differences observed ( $\alpha = 0.05$ ). Moments for both genders increased linearly with increasing sled acceleration.

**Table 12. Gender Specific Peak Neck  $M_y$  Moment Responses (3.0 lb helmet)**

Sled Accel (G)	Male Average (in- lbs)	Female Average (in- lbs)	Percent Difference	P
6 (T2)	270.73 ± 46.74	275.33 ± 63.42	1.7%	0.84
8 (L)	357.63 ± 66.61	346.66 ± 72.04	-3.1%	0.69
10 (F)	516.20 ± 138.94	489.06 ± 90.42	-5.3%	0.76

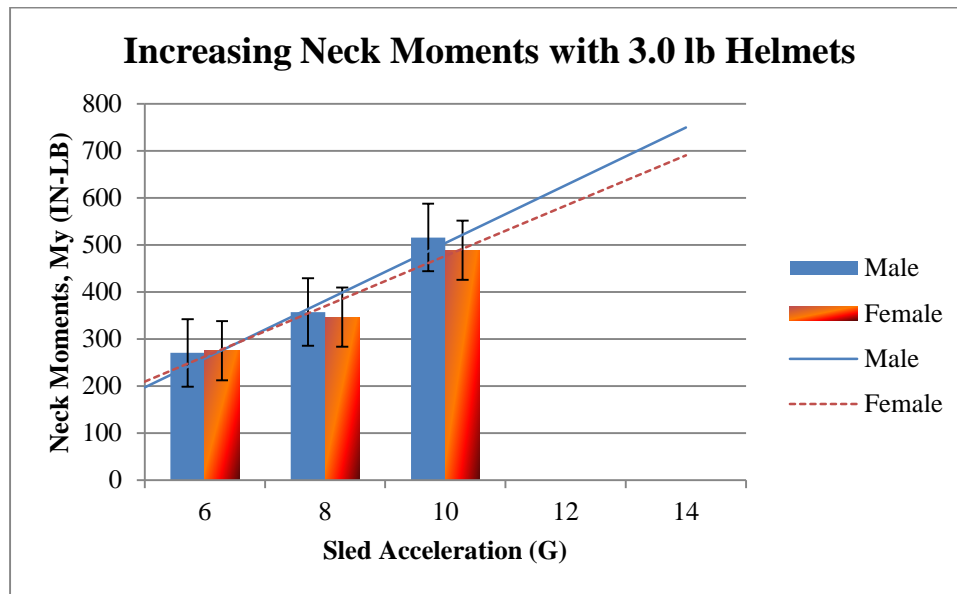


**Figure 13. Neck  $M_y$  Moments as a Function of Sled Acceleration Level (3.0 lb Helmet)**

#### 4.4 Pre-Impact Headrest Bracing Loads

Differences among average peak pre-impact headrest bracing loads were examined to evaluate the effects of subject bracing loads exerted on the contoured headrest (Table 13 and Figure 14). For this study, subjects were instructed to brace at their maximum against the headrest just prior to and during sled acceleration; the data show that the subjects braced at different levels with males demonstrating greater variability than females. Overall, males braced at higher levels than females with statistical significance for all helmet conditions but the 4.5 lb helmet. Neither males nor females showed any trends of varying their bracing levels with increasing helmet weight.

**Table 13. Headrest Bracing Loads for 8 G Sled Accelerations**

Helmet Weight (lbs)	Male Average (lbs)	Female Average (lbs)	Percent Difference	P
3.0 (L)	48.23 ± 16.60	36.33 ± 9.35	-24.7%	0.04
3.5 (V)	47.52 ± 13.98	37.25 ± 10.00	-21.6%	0.05
4.0 (B)	52.70 ± 19.47	33.93 ± 8.17	-35.6%	0.00
4.5 (D)	47.22 ± 11.08	39.90 ± 9.64	-15.5%	0.12

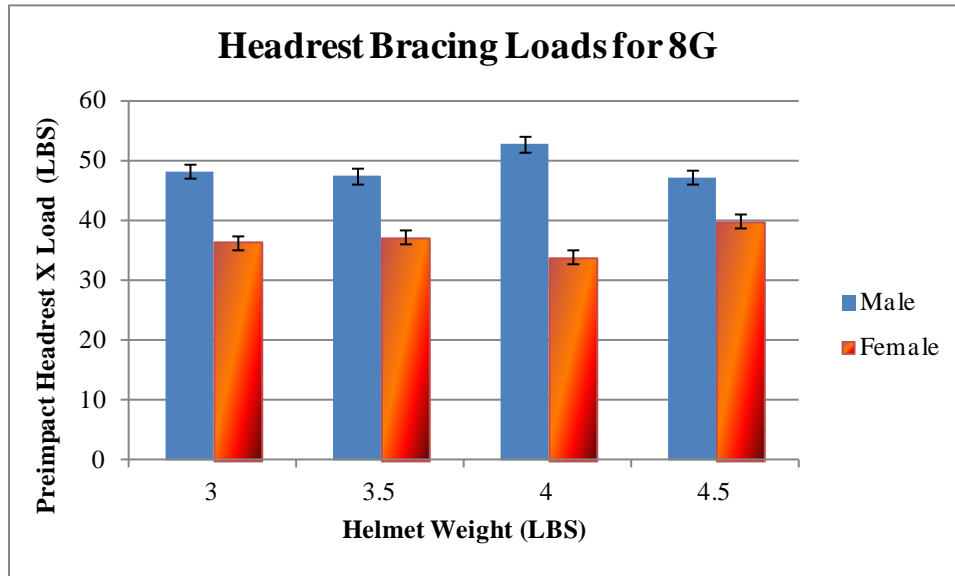


**Figure 14. Pre-impact Headrest Load with Increasing Helmet Weight (at 8G)**

Overall, there was a very large range of bracing among the subjects (Table 14). For all test conditions, the average pre-impact headrest bracing load for males was 48.75 lbs, with a maximum of 124.05 lbs and minimum of 11.18 lbs. The average pre-impact headrest bracing load for females was 37.21 lbs, with a maximum of 64.92 lbs and minimum of 12.06 lbs. Although males demonstrated the highest bracing loads overall, variability as demonstrated by the standard deviation (SD) for the males was almost twice that of females.

**Table 14. Mean and SD of all Headrest Bracing Loads**

Gender	Maximum Brace (lbs)	Average Brace (lbs)	Minimum Brace (lbs)
Male	124.05	48.75 ± 16.03	11.18
Female	64.92	37.21 ± 9.28	12.06

#### 4.5 Effects of Subject Bracing

A total of 7 subjects completed cell LR, which called for the subjects to brace at a lower than normal pre-impact level of 20 ± 5 lbs (moderate brace). For all other cells, subjects were instructed to brace at their maximum headrest load (full brace). As seen in Table 15, those

subjects who completed the moderate bracing tests generated slightly less than half the average pre-impact headrest force (25.9 lbs) when compared to the full brace (58.0 lbs).

**Table 15. Comparison of Headrest Loads in Moderate and Full Bracing Tests**

Bracing Level	Number of Subjects	Average (lbs)
Moderate Brace	7	25.87 ± 6.56
Full Brace	7	57.95 ± 12.43

Figures 15-17 compare moderate brace tests to full brace tests for individual subjects. In both cases the subjects wore a 3.0 lb helmet and were accelerated at 8 G. The results from cell LR, which required the subjects to brace moderately before impact, were compared to the results of cell L for the same subjects, which called for a full brace.

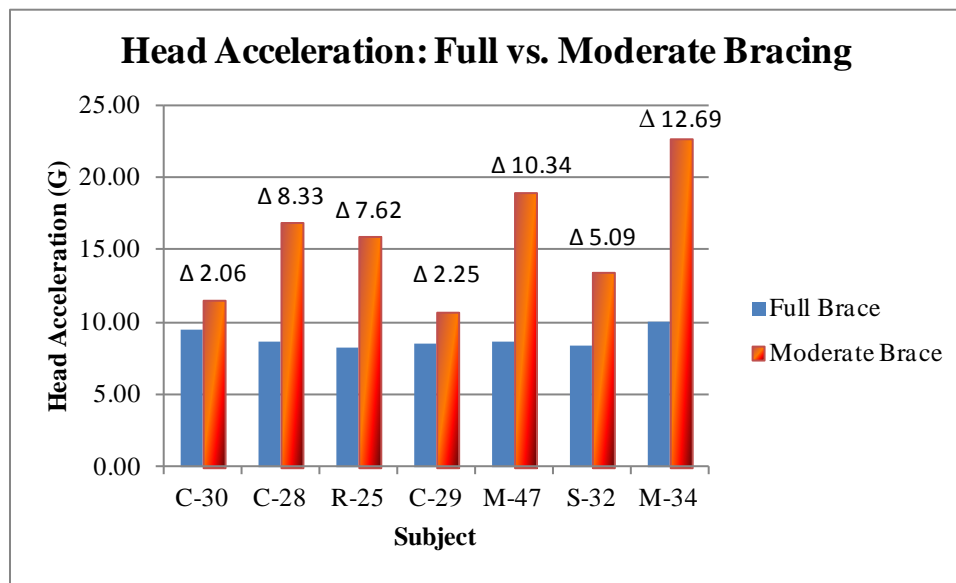


**Figure 15. Bracing Effects on Head X-Axis Acceleration at 8 G with 3.0 lb Helmet**

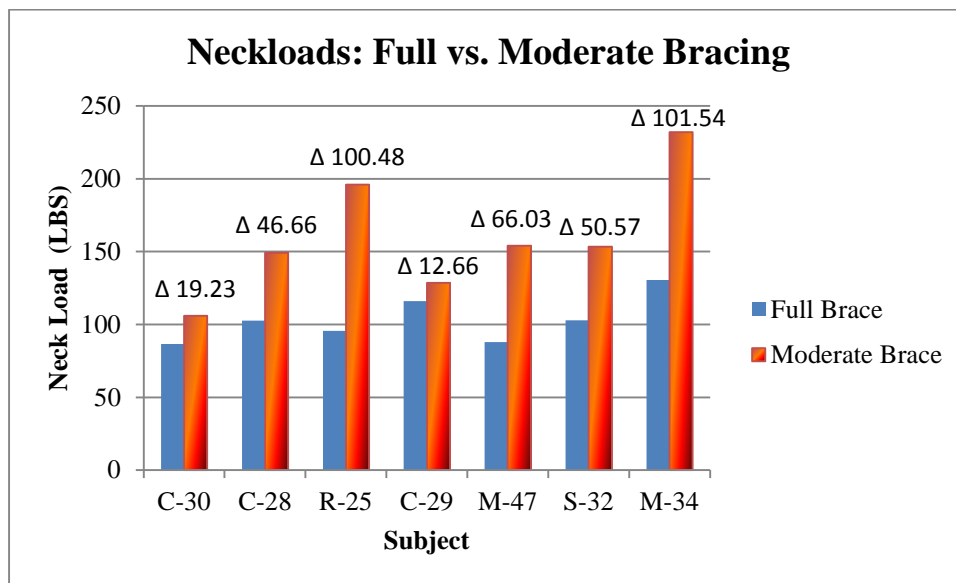


Figure 16. Bracing Effects on Neck X-Axis Load at 8 G with 3.0 lb Helmet

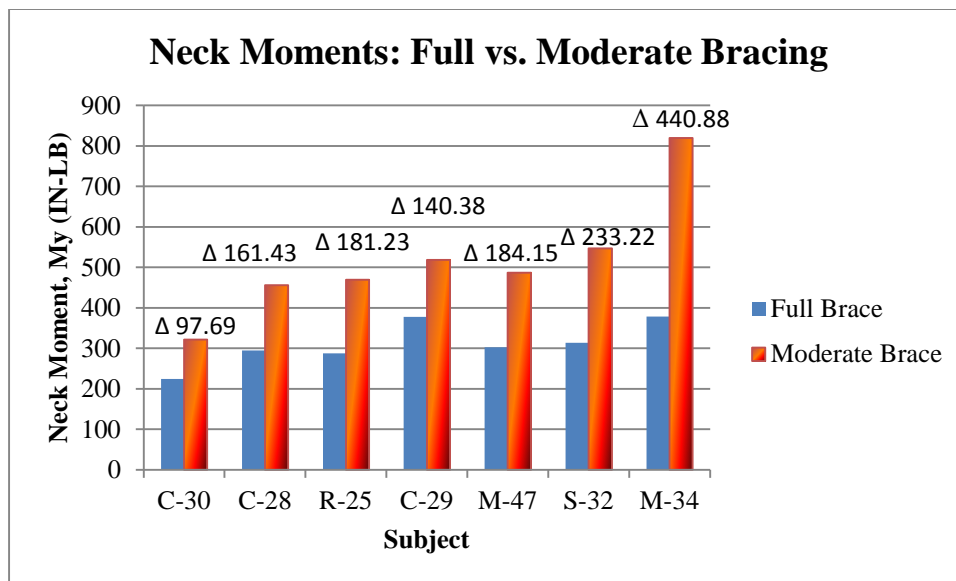


Figure 17. Bracing Effects on Neck Moments ( $M_y$ ) at 8 G with 3.0 lb Helmet

All of the subjects who were accelerated while performing a moderate brace averaged higher head accelerations, neck loads and neck moments than they did when performing a full brace. On average, moderately bracing subjects experienced head accelerations, neck loads and neck moments that were respectively 1.78, 1.55 and 1.64 times higher than what they experienced when bracing fully.

#### 4.6 Head Displacements

Comparisons were made for displacements in the X-axis, Z-axis and the overall resultant as measured at the mouth (Table 16). Each subject wore an instrumented mouthpiece to obtain the data. The resultant displacements were calculated by taking the square root of the sum of squares of the X, Y and Z displacements, done on a point-by-point basis. The Y-values were negligible and had little effect on the resultants. In all cases, females demonstrated higher

resultant displacements then did males. However, no statistical significance was determined between genders, although gender differences in cell W were close to statistical significance ( $p = 0.06$ ). In all cases, except male mean displacements between 4.0 and 4.5 lb helmets, displacements increased as helmet weight increased for both genders at a constant 8 G sled acceleration (Table 16, Figure 18). In addition, head displacements also increased for both males and females as sled acceleration increased for a constant 4.5 lb helmet weight (Table 16).

**Table 16. Gender Comparison of Resultant Displacements at Mouth**

Mean Peak Mouth Resultant Displacement (in)*					
Sled Accel (G)	Helmet Weight (lbs)	Male Average (in)	Female Average (in)	Percent Difference	P
8	3.0 (L)	8.24 ± 3.06	8.94 ± 1.56	8.5%	0.48
	3.5 (V)	8.75 ± 2.81	9.41 ± 1.60	7.5%	0.50
	4.0 (B)	9.85 ± 2.25	9.99 ± 1.02	1.4%	0.83
	4.5 (D)	9.46 ± 2.28	10.38 ± 1.12	9.7%	0.30
7	4.5 (W)	6.62 ± 1.04	7.72 ± 1.32	16.6%	0.06
6	4.5 (C)	5.23 ± 2.59	6.24 ± 1.42	19.3%	0.25

\* Resultant displacements were calculated by taking the square root of the sum of squares of the X, Y and Z displacements, done on a point-by-point basis

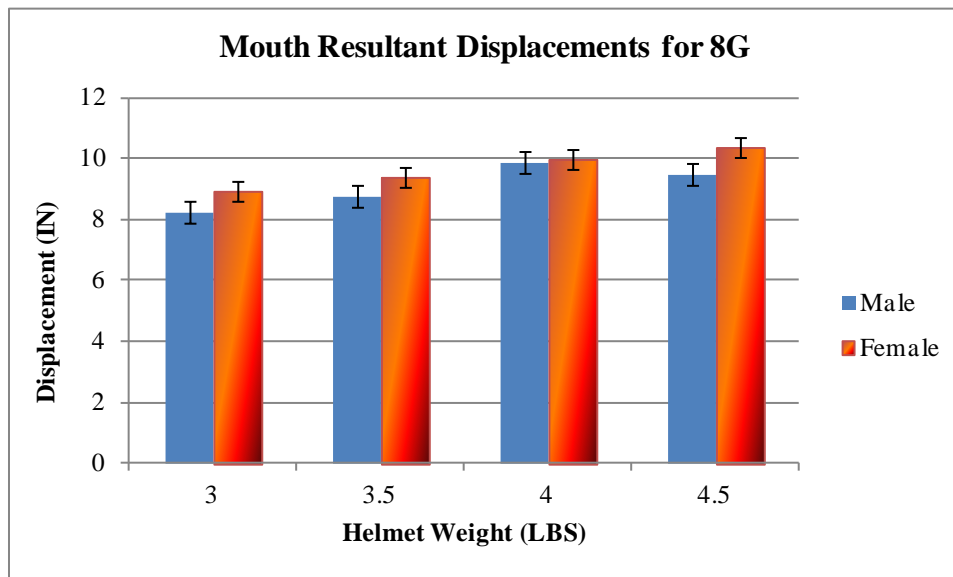


**Figure 18. Gender Comparison of Peak Resultant Displacement as a Function of Helmet Weight (at 8 G)**

#### 4.7 Discomfort Incidences (Subjective)

Another important area of investigation was the incidence of neck and back discomfort, which was compiled to better understand potential injury threshold limits and how these might differ between the genders. At the end of each test, the subject reported whether the conditions under which he or she was tested caused any discomfort or pain. The symptoms were categorized as either “mild”, “moderate” or “severe” which are defined below:

Mild: pain or discomfort described as “slight”, “mild” or “dull” and went away within 48 hours

Moderate: pain or discomfort language that suggested the injury was more than mild and/or was a specific injury (e.g. pinched nerve) and/or lasted more than 48 hours

Severe: pain, discomfort or incidences that resulted in the subject being removed from the study (or had strong considerations to discontinue) and/or an x-ray was required and/or the subject displayed whiplash symptoms.

The majority of symptoms were mild—particularly involving temporary neck stiffness and/or soreness. On average, females experienced higher rates of discomfort incidences per capita. Table 17 (duplicates and outliers included) shows that females reported more incidences of mild through severe discomfort in their back and neck than did males (27 vs. 10), although females ran fewer tests. Overall, females experienced neck and/or back discomfort in 23.3% of their test runs, whereas males experienced a 6.5% incidence rate of discomfort. None of the discomfort incidents were considered serious by the Medical Monitor.

**Table 17. Discomfort Incidences with Respect to Gender (Neck and Back)**

Gender	Neck			Back			Total	Test Runs	% Discomfort
	Mild	Mod.	Sev.	Mild	Mod.	Sev.			
Male	3	1	0	3	3	0	10	154	6.5%
Female	13	5	3	5	0	1	27	116	23.3%
<b>Total</b>	16	6	3	8	3	1	37	270	13.7%

Table 18 (duplicate test runs and outliers included) shows the incidences of discomfort in the neck and back categorized by gender, helmet weight, and sled acceleration. Seven (7) additional incidents were included where the comments likely referred to the back or neck but were not specific enough to be linked to one or the other. These cases and the corresponding subject identification number and test cell are provided below:

Males

M-45 (L/L1): “a little stiff day after”

C-29 (X/X1): “a little stiff, better after 72 [hours]”

M-47 (F): “subject had major soreness and reservations about continuing study”

H-25 (F): “subject had severe soreness and reservations about continuing study”

Females

S-34 (L/L1, V/V1, W/W1): “slight stiffness”

Males participated in significantly more 10 G tests than females (35 versus 16 tests). In addition, three males were able to complete cell M (10 G, 3.5 lb helmet) while no females (or the Medical Monitor) felt comfortable running tests under these conditions. Of the subjects willing/able to undergo 10 G tests, however, 7 out of 35 males (20.0%) experienced a discomfort incident while 3 out of 16 females (18.8%) experienced discomfort incidences.

**Table 18. Discomfort Incidences with Respect to Gender, Helmet Weight, and Sled Acceleration (Neck and Back – Includes General Symptoms)**

Gen.	6G			7G	8G				10G				Tot.
	3lb (T2)	4lb (A2)	4.5lb (C)	4.5lb (W)	3lb (L, LR)	3.5lb (V)	4lb (B)	4.5lb (D)	0lb (E)	2lb (X)	3lb (F)	3.5lb (M)	
M	0/11	0/17	1/17	0/10	3/21	0/13	3/16++	0/14	0/13	4/8++	2/11**	1/3	14/154
F	2/13	1/17*	1/11	5/11+	7/13*+	3/11+	8/14***+	0/10	1/7	1/6	1/3+	0/0	30/116
	2/24	1/34	2/28	5/21	10/34	3/24	11/30	0/24	1/20	5/14	3/14	1/3	44/270

+ Moderate discomfort incidences.

\* Severe discomfort incidences.

Discomforts that did not refer to the neck or back were not included above. These incidents were primarily referred to as leg, groin, and/or shoulder discomforts which were generally caused by the friction and/or compression of the restraint straps during acceleration.

## 5.0 DISCUSSION

**Acceleration Response:** In general, head x-axis accelerations increased linearly with increasing sled acceleration and constant helmet weight. This was not as well defined when helmet weight was increased and sled acceleration was held constant. Head accelerations did increase linearly when helmet weight was increased from 3.0 to 4.0 lb in males, and 3.0 to 3.5 lb in females. These increases, however, were small compared to those observed with increasing sled accelerations, and head acceleration actually decreased with higher helmet weight for both genders under some conditions (4.0 to 4.5 lb helmet for males, and 3.5 to 4.0 lb helmet for females). This suggests that subjects are capable of compensating for increased head accelerations (likely due to musculature during bracing) caused by heavier helmets far better than they are with forces caused by increasing sled acceleration. Regarding gender differences, female subjects tended to have higher head accelerations and resultant displacements than did the male subjects. One explanation could be that females, on average, have smaller neck circumferences and less neck strength than males. On impact, both males and females brace their heads, but males are likely better able to hold the brace throughout the impact duration due to their stronger neck muscles. A stronger brace means that less energy is dissipated in the overall acceleration of the head, and less flexion and lower accelerations normally result. This was demonstrated by the males generating higher pre-impact headrest loads (i.e. headrest bracing loads) resulting in lower corresponding head accelerations than females under most conditions.

**Neck Loads:** Females tended to have higher head accelerations, but experienced neck loads comparable to males. This may be because males have a larger combined helmet, head and neck weight than females, which would offset any gender differences caused by the females' higher head accelerations.

Although male and female subjects experienced similar neck loads, fewer females tolerated the higher sled accelerations and heavier helmet-weighted tests than males. This tends to corroborate the current consensus among DoD researchers that lower neck load limits are appropriate for females, as seen in the Air Force JSF Neck Injury Criteria (NIC) [5]. The JSF NIC limits for small females were established at 165 lbs in shear, so according to the extrapolated plots in Figure 10, females would exceed this limit at only 12 G of sled acceleration while wearing a 3.0 lb helmet. Females tend to have lower neck strength making them less able to mitigate head accelerations with headrest bracing. In addition, females on average have smaller cervical cross-sectional areas than males, which would be expected to contribute to greater cervical stress during neck loading. This could lead to increased risk of neck injury as compared to males under the same conditions [3]

As expected, neck loads increased linearly with increasing impact acceleration. This linearity was extrapolated out to include higher acceleration levels and heavier helmets. Using this method the predicted shear loads at 15 G with 4.5 lb helmet would be within the range of 250-300 lbs which would not be tolerated well by most individuals. The possibility also exists for non-linear loading trends at the higher impact accelerations, in which case the neck loads could be even larger than estimated here.

The neck loads from this study were compared to known injury limits set by previous cadaver studies conducted in the same axis. In 1971 Mertz and Patrick conducted a study that involved a human volunteer and four cadaver specimens on an impact sled track [4]. The cadavers were

accelerated up to 14.2 G with 5.0 lbs of added helmet weight. A maximum shear load of 473.0 lbs was observed in the cadaver specimens without any observable ligamentous, disc, or bone damage as noted from x-ray analysis of the neck structures. These cadaver neck loads were higher than the extrapolated neck loads for our human subjects under comparable conditions of 15 G seat acceleration and 4.5 lb helmet weight. The difference is probably due to our subjects being able to brace their heads against the headrest, thus decreasing their maximum neck load. The Mertz and Patrick study also employed a headrest that was extended several inches forward which likely contributed to greater head rotation and acceleration.

There is concern about injury risk due to neck loads that fall between the Mertz and Patrick cadaver injury threshold of 473 lbs and our experimental maximum tolerable levels of 189 lbs (females) and 265 lbs (males), due to the incidence of discomfort and pain reported by some of our subjects when experiencing neck loads at or below these levels. Based on our subjects' symptoms and depending on subject anthropometry and gender, it is conceivable that severe pilot whiplash-type injuries could occur within this range of neck loads, particularly during the extreme conditions of the ejection parachute opening shock phase. Although it is unlikely that permanently debilitating neck injury would be incurred at these levels for mid or large crewmembers, these injuries could nonetheless cause incapacitation of the pilot over an extended period. Small female crewmembers would appear to be at greater risk of more serious neck injury at these higher levels, as evidenced by their lower bracing levels, lower discomfort thresholds, and greater estimated cervical stress.

**Neck Moments:** The subjects in this study demonstrated a wide range of neck moments. In general, neck moments tended to increase with increases in helmet weight and sled acceleration level. However, there were some exceptions where the subjects were able to offset potentially higher moments with better bracing, as evidenced by male subjects on average having very similar moments with the 4.5 lb helmet than the 4.0 helmet and females having slightly lower moments with the 4.0 lb helmet than the 3.5 lb helmet during 8 G tests. This was not necessarily demonstrated in the maximum headrest bracing table since the subjects tended to brace at similar levels for all helmets. However, it is possible that the subjects may have maintained their brace for longer durations during some tests, thus offsetting the moments in these cases. In general, males and females generated similar neck moments, although males tended to experience slightly higher moments than females. This is likely due to the fact that males, on average, have larger heads and necks than do females, thus resulting in more mass at the end of the moment arm. This became more apparent during tests which tended to generate greater moments (high sled acceleration, heavy helmet with forward cg). Pre-impact bracing had a significant effect on neck moments as demonstrated by the fact that the subjects generated lower neck moments when they performed a pre-impact full brace as compared to a moderate brace. Better bracing resulted in lower neck loads which contributed to lower moments.

**Effects of Subject Bracing:** Interestingly, the subjects increased their static pre-impact headrest (i.e. bracing) loads with increasing sled acceleration levels. The subjects were informed of the impending level before each test; therefore, motivation could have been the cause for the increase in bracing level. The bracing level had an obvious effect on dynamic neck loads as demonstrated by the lower dynamic loads generated during the full brace cell compared to the moderate brace cell. However, since only one female participated in the moderate bracing cell, results from this observation are based on a primarily male population. In the remaining cells requiring a full brace, the female subjects braced at lower levels on average than the males, but

did not necessarily experience higher neck loading, due to their smaller head mass. In general, the bracing reduced the head motion relative to the seat, thus mitigating the head accelerations and corresponding neck loads and moments. Although the potential for neck muscle strain or injury due to excessive bracing has not yet been investigated, this did not appear to be an issue during the maximum bracing cells.

Some of the subjects had difficulty adequately holding their braces during the impact when asked to brace at less than their maximum level. It appears that maximum bracing acts to offset neck loading during impact, and is more effective in preventing neck soreness than moderate bracing at a targeted level. This appears to be true regardless of the level of the subject's maximum bracing. We therefore recommend that pilots perform a maximum brace during the catapult phase of ejection as well as just prior to the opening of their parachute.

***Discomfort Incidences (Subjective):*** Temporary neck and/or back discomfort (primarily stiffness and soreness) were reported in 13.7% of the tests, generally at higher acceleration levels with heavier helmets. Females were more likely than males to experience these symptoms since they generated neck loads that were comparable to males under the same conditions, but their established load tolerance limits were much lower. Three male subjects completed cell M (10 G, 3.5 lb helmet) and provided some type of commentary related to discomfort. The helmet weight was subsequently limited to 3.0 lbs during 10 G runs. We recommend closely monitoring future -x axis tests where sled accelerations exceed 10 G and/or helmet weights exceed 3.5 lbs.

## 6.0 CONCLUSIONS

This test program demonstrated the acceleration response and neck loading on human volunteer subjects wearing forward-weighted helmets during horizontal impact accelerations. In general, the subjects tolerated sled input accelerations up to 8 G with 4.5 lb helmets and up to 10 G with 3.0 lb helmets without significant incident, but pain/discomfort thresholds began to be reached when the weight was increased to 3.5 lbs at 10 G. While females more often generated higher head accelerations, males tended to have larger and heavier heads, so the overall neck loads demonstrated little or no gender difference. However, females tend to have smaller vertebral cross-sectional areas than males so they would be likely to generate greater cervical stress, possibly leading to increased risk of neck injury as compared to males under comparable conditions. In addition, the female subjects were on average unable to sustain as forceful a brace during pre-impact as the males, which may account for their higher head accelerations and higher percentage of reported adverse effects. Firm bracing of the head against the headrest can act to mitigate the head accelerations and corresponding neck loads and moments. Consequently, individual bracing abilities—regardless of gender or anthropometry, should be taken into account when assessing risk of injury.

The extrapolated data indicate that under extreme conditions as seen during the parachute opening phase of aircraft ejection where seat decelerations can approach 15 G, mid-size and large male pilots would likely not incur significant permanent neck injury. However, there is concern that severe whiplash or other neck trauma could occur at these levels, particularly with forward-loaded helmet weights greater than 4.5 lbs. In particular, small females would be at greater risk of serious injury under these conditions. The likelihood and severity of injury would depend on the pilot's gender, anthropometry, and bracing techniques.

## 7.0 REFERENCES

1. Buhrman, J.R., C.E. Perry, and F.S. Knox III (1994). Human and Manikin Head/Neck Response to +Gz Acceleration When Encumbered by Helmets of Various Weights. *Aviation, Space, and Environmental Medicine*, 65, 1086-1090.
2. Buhrman, J. R., C.E. Perry, and S.E. Mosher (2000). A Comparison of Male and Female Acceleration Responses During Laboratory Frontal –Gx Axis Impact Tests. Air Force Technical Report AFRL-HE-WP-TR-2001-0022.
3. Gallagher H.L., Buhrman J.R., Perry C.E., Mosher S.E., and Wilson D.D. (2007). An Analysis of Vertebral Stress and BMD During +Gz Accelerations. Air Force Technical Report AFRL-HE-WP-TR-2007-0085.
4. Mertz, H.J. and L.M. Patrick (1971). Strength and response of the human neck. Proceedings of the Fifteenth Stapp Car Crash Conference, Society of Automotive Engineers, Warrendale, PA: SAE.
5. Nichols, J.P. (2006). Overview of Ejection Neck Injury Criteria, Proceedings of the 44<sup>th</sup> Annual SAFE Symposium, Reno.
6. Perry, C.E. (1998). The Effect of Helmet Inertial Properties on Male and Female Head Response During +Gz Impact Accelerations, *SAFE Journal*, 28(1), 32-38.
7. Perry, C.E. and Buhrman J.R. (1997). Head Mounted Display (HMD) Head and Neck Biomechanics. In: Head Mounted Displays: Designing for the User, 6, 147-174. J.E. Melzer and K. Moffitt (Eds.), New York: McGraw-Hill.
8. Perry, C.E. and Buhrman J.R. (1996). Effect of Helmet Inertial Properties of the Biodynamics of the Head and Neck During +Gz Impact Accelerations. *SAFE Journal*, 26(2), 34-41.
9. Perry, C.E., Buhrman J.R., Doczy E.J. and Mosher S.E. (2003). Evaluation of the Effects of Variable Helmet Weight on Human Response During Lateral +Gy Impact. AFRL-HE-WP-TR-2004-0013.
10. Perry, C.E., Rizer A.R., Smith J.S., and Anderson B. (1997). Biodynamic Modeling of Human Neck Response During Vertical Impact. *SAFE Journal*, 27(3), 183-191.
11. Pint, S. M. (2003). Evaluation of the Human Response to Upper Torso Retraction with Added Helmet Weight. Abstract presented at AsMA Annual Scientific Meeting, San Antonio TX.

**APPENDIX A: Summary Statistical Data Sheet**

## Summary Data Sheet: Results from Two-Tailed Two-Sample t-tests and Cohen's d Differences between Group Means

Dependent Variable	Male		Female		Mean Diff	Two-Tailed Two-Sample t-test			n		Cohen's d
	Mean	SEM	Mean	SEM		DF	t	p	M	F	
Head Acceleration Cell L (8G) Helmet Weight (3.0lb) <sup>1</sup>	9.81	0.43	11.00	0.33	-1.19	24	2.14	0.0423	14	12	0.85
Head Acceleration Cell V (8G) Helmet Weight (3.5lb)	10.11	0.42	11.66	0.51	-1.55	22	2.37	0.0270	13	11	0.97
Head Acceleration Cell B (8G) Helmet Weight (4.0lb)	11.10	0.58	10.80	0.45	0.30	27	0.39	0.6967	16	13	0.15
Head Acceleration Cell D (8G) Helmet Weight (4.5lb)	10.11	0.46	10.99	0.50	-0.89	21	1.27	0.2167	14	9	0.55
Head Acceleration Cell C (6G) Helmet Weight (4.5 lb)	6.75	0.33	7.21	0.23	-0.46	25	1.04	0.3071	16	11	0.43
Head Acceleration Cell W (7G) Helmet Weight (4.5 lb)	7.94	0.21	9.45	0.33	-1.51	19	3.75	0.0013	10	11	1.66
Head Acceleration Cell T2 (6G) Helmet Weight (3.0 lb) <sup>2</sup>	6.58	0.20	7.38	0.31	-0.80	23	2.31	0.0302	13	12	0.91
Head Acceleration Cell F (10G) Helmet Weight (3.0 lb)	14.14	0.86	14.80	1.88	-0.67	12	0.35	0.7310	11	3	0.22
Neck X Loads Cell L (8G) Helmet Weight (3.0 lb) <sup>3</sup>	111.92	4.55	103.15	3.73	8.76	24	1.46	0.1578	14	12	0.58
Neck X Loads Cell V (8G) Helmet Weight (3.5 lb)	119.09	4.62	115.00	5.26	4.09	22	0.59	0.5640	13	11	0.24
Neck X Loads Cell B (8G) Helmet Weight (4.0 lb)	130.32	6.48	117.72	5.18	12.60	27	1.47	0.1535	16	13	0.56
Neck X Loads Cell D (8G) Helmet Weight (4.5 lb)	130.17	5.25	129.68	7.68	0.50	21	0.06	0.9565	14	9	0.02
Neck X Loads Cell C (6G) Helmet Weight (4.5 lb)	88.03	4.01	86.11	3.98	1.92	25	0.33	0.7466	16	11	0.13
Neck X Loads Cell W (7G) Helmet Weight (4.5 lb)	106.90	4.86	115.21	6.99	-8.32	19	0.96	0.3501	10	11	0.42
Neck X Loads Cell T2 (6G) Helmet Weight (3 lb) <sup>4</sup>	81.11	3.19	71.84	2.22	9.26	23	2.65	0.0143	13	12	1.07
Neck X Loads Cell F (10G) Helmet Weight (3 lb)	160.66	13.51	157.36	27.75	3.31	12	0.11	0.9128	11	3	0.07
Neck Moments Cell L (8G) Helmet Weight (3.0 lb) <sup>5</sup>	357.63	17.80	346.66	20.80	10.97	24	0.40	0.6904	14	12	0.16
Neck Moments Cell V (8G) Helmet Weight (3.5 lb)	379.58	23.18	395.33	28.49	-15.74	22	0.43	0.6691	13	11	0.18
Neck Moments Cell B (8G) Helmet Weight (4.0 lb)	435.58	30.36	408.29	24.50	27.28	27	0.68	0.5044	16	13	0.26
Neck Moments Cell D (8G) Helmet Weight (4.5 lb)	435.77	24.89	396.56	14.65	39.22	21	1.17	0.2533	14	9	0.54
Neck Moments Cell C (6G) Helmet Weight (4.5 lb)	325.93	18.69	329.44	20.19	-3.51	25	0.12	0.9016	16	11	0.05
Neck Moments Cell W (7G) Helmet Weight (4.5 lb)	393.31	29.65	397.43	33.29	-4.11	19	0.09	0.9281	10	11	0.04

<sup>1</sup> Male outlier removed

<sup>2</sup> Male outlier removed

<sup>3</sup> Male outlier removed (same as above)

<sup>4</sup> Male outlier removed (same as above)

<sup>5</sup> Male outlier removed (same as above)

Neck Moments Cell T2 (6G) Helmet Weight (3 lb) <sup>6</sup>	270.73	15.58	275.33	18.31	-4.60	23	0.21	0.8374	13	12	0.08
Neck Moments Cell F (10G) Helmet Weight (3 lb)	516.20	41.89	489.06	52.21	27.14	12	0.32	0.7578	11	3	0.23
Bracing Load Cell L (8G) Helmet Weight (3.0 lb)	48.23	4.29	36.33	2.70	11.90	25	2.21	0.0363	15	12	0.88
Bracing Load Cell V (8G) Helmet Weight (3.5 lb)	47.52	3.88	37.25	3.02	10.27	22	2.03	0.0543	13	11	0.85
Bracing Load Cell B (8G) Helmet Weight (4.0 lb)	52.70	4.87	33.93	2.26	18.76	27	3.24	0.0031	16	13	1.26
Bracing Load Cell D (8G) Helmet Weight (4.5 lb)	47.22	2.96	39.90	3.21	7.33	21	1.62	0.1192	14	9	0.71
Sled Accel (8G) Resultant Displacement (3lb Helmet) Cell L	8.24	0.79	8.94	0.45	-0.70	25	0.72	0.4811	15	12	0.29
Sled Accel (8G) Resultant Displacement (3.5lb Helmet) Cell V <sup>7</sup>	8.75	0.81	9.41	0.48	-0.66	21	0.69	0.5000	12	11	0.29
Sled Accel (8G) Resultant Displacement (4.0lb Helmet) Cell B <sup>8</sup>	9.85	0.58	9.99	0.28	-0.14	26	0.21	0.8330	15	13	0.08
Sled Accel (8G) Resultant Displacement (4.5 lb Helmet) Cell D <sup>9</sup>	9.46	0.61	10.38	0.40	-0.92	20	1.06	0.3011	14	8	0.51
Sled Accel (7G) Resultant Displacement (4.5lb Helmet) Cell W <sup>10</sup>	6.62	0.33	7.72	0.44	-1.10	17	2.04	0.0576	10	9	0.93
Sled Accel (6G) Resultant Displacement (4.5lb Helmet) Cell C	5.23	0.67	6.24	0.43	-1.00	25	1.17	0.2542	16	11	0.48

<sup>6</sup> Male outlier removed (same as above)

<sup>7</sup> Male subject data set does not exist

<sup>8</sup> Male subject data set does not exist

<sup>9</sup> Female subject data set does not exist

<sup>10</sup> Two female subject data sets do not exist

## **APPENDIX B: Test Configuration and Data Acquisition System**



## VARIABLE WEIGHTED HELMET G<sub>x</sub> STUDY

Study Number 200301

Prepared under Contract FA8650-04-D-6472

AUGUST 2004

Advanced Information Engineering Services  
A General Dynamics Company  
5200 Springfield Pike, Suite 200  
Dayton, OH 45431

# Test Report

## Variable Weighted Helmet Gx Study (VWHGX)

### Horizontal Impulse Accelerator (HIA) Tests

#### **Introduction**

General Dynamics has prepared this report for the Air Force Research Laboratory, Human Effectiveness Directorate, Biomechanics Branch under Air Force contract FA8650-04-D-6472. It describes the test facility, test configurations, data acquisition and analysis, and instrumentation procedures used for the Variable Weighted Helmet Gx (VWHGX) Study (Study 200301). A series of impact tests were performed on the Horizontal Impulse Accelerator (HIA) located in Bldg. 824 at Wright-Patterson AFB. An Advanced Dynamic Anthropomorphic Manikin (ADAM) manikin weighing 218 lbs was used in this test program.

#### **Test Facility**

##### **Horizontal Impulse Accelerator**

The AFRL/HEPA HIA (Figure A-1) was used for all of the tests. The Horizontal Impulse Accelerator (HIA) system consists of a 24-inch HYGE actuator, a 4-foot x 8-foot test sled, and a 240-foot track. The HYGE actuator is a hydraulic/pneumatic system manufactured by the Bendix Corporation. It has front and rear cylinder sections, each with a hydraulically controlled floating piston for controlling the volumes in the gas pressure chambers. The energy of high-pressure gas in the load chamber propels the thrust piston to create the acceleration pulse for the test sled. The system is armed by pressurizing the set chamber with nitrogen to seal the thrust piston to the orifice plate. Then, the load chamber is pumped up with compressed air approximately six times the set pressure depending on test conditions. Trigger pressure breaks the orifice seal and exposes the full surface area of the thrust piston to the load pressure for test initiation. The geometric profile of the metering pin attached to the face of the thrust piston varies the orifice area and controls the shape of the acceleration pulse. Various acceleration profiles (half-sine, trapezoidal, etc.) are available by changing the metering pin. For these tests, metering pin number 11 was used to approximate a half-sine acceleration profile with 150ms pulse duration.

The HIA system simulates impact phenomena by accelerating a test payload from rest. The test subject experiences dynamic loads equivalent to the forces experienced during an actual impact. There are several laboratory control advantages in having the initial position at rest, which include: accurate positioning of the subject prior to the test; no extraneous forces present prior to the test; precise control of test initiation and data collection systems; and rapid, repeatable reset of test conditions.



## Figure 1. HIA Facility

A total of 541 tests (human and manikin) were completed on the HIA from 3 February 2003 to 18 June 2004. Other program documentation information is found in Table A-1.

**Table 1. Program Documentation Information**

<b>Equipment</b>	<b>ID</b>
Facility	HIA
Metering Pin Number	11
Seat Fixture	40G
Seat Cushion	None
Harness	PCU-16/P, 15/P, IMPACT
Helmet	See Test Matrix
Inertia Reel	None
Lap Belt	HBU
Oxygen Mask	Modified 12/P
NVG/HMD	None
Neg-G Strap	None
Headrest Position	Vertical
Seat Pan Position	Horizontal
Seat Back Position	Vertical

### Test Fixture

The 40 G seat fixture was used in the VWHGX study (Figure A-2). For all cells except AA, BB, CC and DD, all subjects (human and manikin) were seated in an upright posture and restrained to the seat using a PCU-15/P or PCU-16/P restraint harness, two shoulder straps, and an HBU lap belt. For cells AA, BB, CC and DD the 40 G seat back was modified to a slightly reclined position (Figure A-3) and an IMPACT restraint harness was used. For all cells the lap belts and shoulder straps were preloaded to  $20 \pm 5$  pounds. A contoured headrest was used for all tests. The headrest was in-line with the seat back. The headrest was mounted in-line with the seat back on all 40 G seat configurations. Beginning on 25 August 2003 the headrest and shoulder strap attachments were made adjustable for each subject (Figure A-4). The seat back angle was 0 degrees with respect to the vertical and the seat pan angle was 0 degrees with respect to the horizontal (except for cell AA, BB, CC and DD). Beginning on 25 June 2003 adjustable foot pedals were added to the configuration (Figure A-5). Velcro foot and hand restraints were applied to limit flail of the lower and upper extremities. Ballast was used on the sled to keep the total weight of the sled and subject constant. The amount of ballast was equal to  $220 \pm 5$  pounds minus the weight of the test subject.

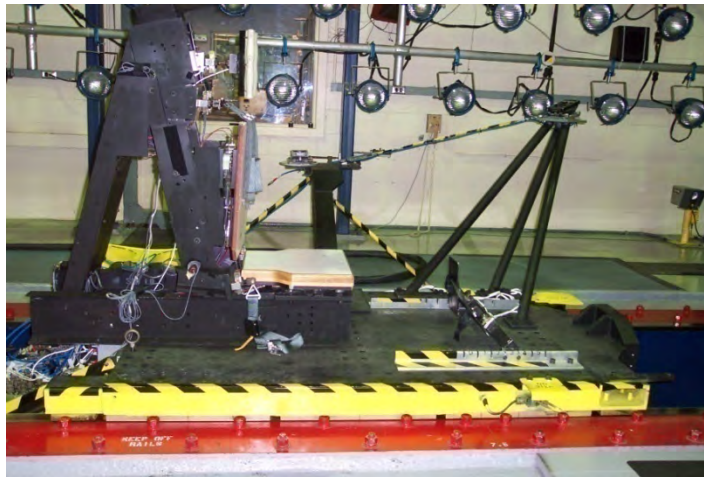


**Figure 2. 40G Seat Configuration**

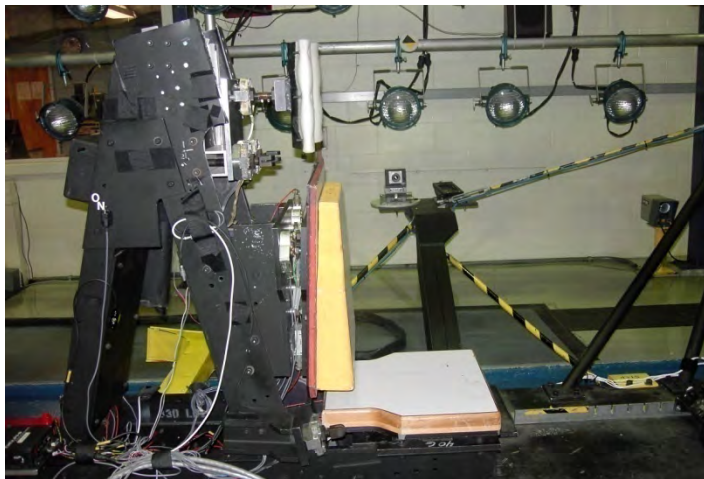


**Figure 3. 40G Seat Configuration for IMPACT Race Harness Cells**

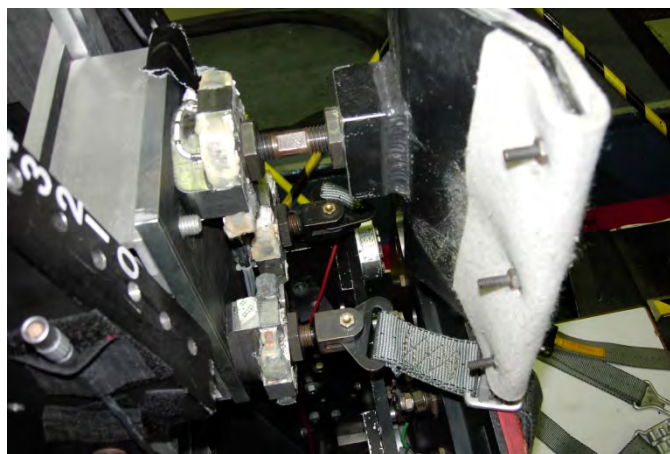


**Figure 4. Adjustable Headrest and Shoulder Straps**



**Figure 5. Adjustable Foot Pedals**

**Test Matrix**

Tests were conducted at the conditions shown in the Test Matrix (Tables A-2 and A-3). Six human subjects were selected to have custom fit earplugs made and participate in the earplug test matrix (Table A-3). Cells AA, BB, CC, and DD were conducted using the IMPACT racing restraint harness at 15 G with a manikin subject. The acceleration waveform for the HIA was an approximate half-sine wave with a peak of 6, 8, 10 or 15G and a time to peak of approximately 75 msec. Several parameter verification tests were completed prior to collection of human data. The Variable Weighted Impact Helmet (VWI) consisted of a modified HGU-55/P flight helmet with additional weights placed on each side of the helmet to maintain symmetry. A modified MBU-12/P oxygen mask was used with the VWI helmet.

**Table 2. Test Matrix for Non-Earplug Subjects**

CELL	PEAK ACCEL. (G)	HELMET	COMMENTS
T	6	3.0 lb VWI	No foot pedals
T2	6	3.0 lb VWI	
A	6	4.0 lb VWI	No foot pedals
A2	6	4.0 lb VWI	
B	8	4.0 lb VWI	
C	6	4.5 lb VWI	
D	8	4.5 lb VWI	
E	10	No helmet	
F	10	3.0 lb VWI	

G	10	4.0 lb VWI	Manikin subjects only
H	10	4.5 lb VWI	Manikin subjects only
L	8	3.0 lb VWI	
LR	8	3.0 lb VWI	Light bracing
M	10	3.5 lb VWI	
V	8	3.5 lb VWI	
W	7	4.5 lb VWI	
X	10	2.0 lb HGU-55/P	

**Table 3. Test Matrix for Earplug Subjects**

CELL	PEAK ACCEL. (G)	HELMET	COMMENTS
C1	6	4.5 lb VWI	
D1	8	4.5 lb VWI	
E1	10	No helmet	
F1	10	3.0 lb VWI	
I1	6	No helmet	Manikin subjects only
J1	6	3.0 lb VWI	
K1	8	No helmet	Manikin subjects only
L1	8	3.0 lb VWI	
LR1	8	3.0 lb VWI	Light bracing

O1	8	3.0 lb VWI	Balaclava with helmet Manikin subjects only
P1	6	Simpson Race	Balaclava with helmet
Q1	6	Bell Race	Balaclava with helmet
R1	8	Simpson Race	Balaclava with helmet
S1	8	Bell Race	Balaclava with helmet Manikin subjects only
V1	8	3.5 lb VWI	
W1	7	4.5 lb VWI	
X1	10	2.0 lb HGU-55/P	
AA	15	IMPACT	No helmet restraint Manikin subjects only
BB	15	IMPACT	Helmet restraint #1 Manikin subjects only
CC	15	IMPACT	Helmet restraint #2 Manikin subjects only
DD	15	IMPACT	Helmet restraint #3 Manikin subjects only

### Instrumentation

Accelerometers and load transducers were chosen to provide the optimum resolution over the expected test load range. Full-scale data ranges were chosen to provide the expected full-scale range plus 50% to assure the capture of peak signals. All transducer bridges were balanced for optimum output prior to the start of the program. The accelerometers were adjusted for the effect of gravity in software by adding the component of a 1 G vector in line with the force of gravity that lies along the accelerometer axis.

The accelerometer and load transducer coordinate systems are shown in Figure A-6. The seat coordinate system is right-handed with the z-axis parallel to the seat back and positive upward. The x-axis is perpendicular to the z-axis and positive eyes forward from the subject. The y-axis is perpendicular to the x- and z-axes according to the right-hand rule. Transducer location measurements are listed in Table A-4. For the measurements listed in Table A-4, the x-axis is defined as eyes forward from the head. The z-axis is defined as vertical. The y-axis is defined by the right-hand rule. Measurements for the load cells were taken at the contact point. The contact point is the point on the load cell where the external force is applied. The measurements for the load cells which anchor the harness were taken at the point where the harness is attached to the load cell. The measurements for the foot pedals (added August 25, 2003) were taken at the point where the foot pedal is attached to the load cell. The foot pedals were measured in position 5 as marked on the adjustment bar. The seat pan accelerometer was measured at the center of the accelerometer block. The headrest load cell was measured at the point where the headrest is attached to the load cell. The headrest-shoulder load cell assembly was measured when the top edge was at position 2. The vertical distance between the headrest positions is one inch. The origin of the coordinate system was located at the midpoint of the low edge of the thin metal strip at the bottom of the seat box. The origin of the seat coordinate system is designated as the seat reference point (SRP). The SRP is at the midpoint of the line segment formed by the intersection of the seat pan and seat back. All vector components

(for accelerations, angular accelerations, forces, moments, etc.) were positive when the vector component (x, y and z) was in the direction of the positive axis.

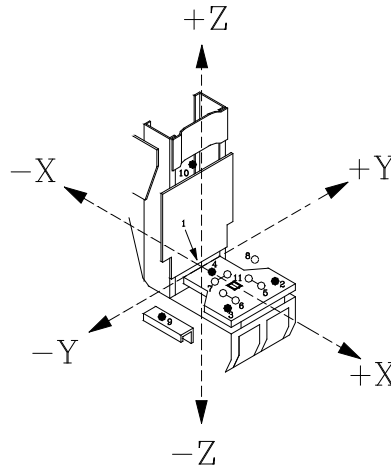


**Figure 6. Coordinate System**

**Table 4. Transducer Location Measurements**

Transducer Measurements 16-Jan-03

Description	X (mm)	Y (mm)	Z (mm)
SRP	0.0	0.0	0.0
Left Lap	44.5	228.0	-50.6
Right Lap	44.5	-235.8	-50.6
Headrest	-121.1	0.9	815.1
Left Shoulder	-80.7	51.4	661.0

Right Shoulder	-80.7	-72.8	662.1
Left Seat Pan X	343.9	157.1	-79.8
Right Seat Pan X	340.9	-149.9	-79.8
Seat Pan Y	221.9	51.5	-79.8
Left Seat Pan Z	445.8	128.0	-61.0
Right Seat Pan Z	447.1	-127.4	-61.0
Center Seat Pan Z	159.9	4.2	-61.0
Seat Pan Accel	346.5	4.2	-119.5
Left Foot Pedal	1157.5	151.8	-190.6
Right Foot Pedal	1157.5	-151.0	-191.1
Top Left Seat Back X	-38.3	138.7	444.6
Top Right Seat Back X	-38.3	-159.5	440.1
Bottom Seat Back X	-38.3	-50.2	133.1
Top Seat Back Y	-53.3	-60.0	443.1
Seat Back Z	-53.3	-8.7	371.4
Bottom Seat Back Y	-53.3	83.2	239.2

Transducer Measurements 26-Aug-03

Description	X (mm)	Y (mm)	Z (mm)
SRP	0.0	0.0	0.0
Headrest	-136.8	-15.0	830.7
Left Shoulder	-101.2	-70.1	670.9
Right Shoulder	-97.9	44.6	666.1

The linear accelerometers were wired to provide a positive output voltage when the acceleration experienced by the accelerometer was applied in the +x, +y and +z directions. The load cells and load links were wired to provide a positive output voltage when the force exerted by the load cell on the subject was applied in the +x, +y or +z direction. The angular Ry rate sensors and accelerometers were wired to provide a positive output voltage when the angular velocity/acceleration experienced by the angular sensor was applied in the +y direction according to the right-hand rule. The manikin lumbar load cells were wired to provide a positive output voltage when the force exerted by the load cell on the lumbar was applied in the +x, +y or +z direction. The manikin torque transducers were wired to provide a positive output voltage when the torque experienced by the transducer was applied in the +x, +y or +z direction. All transducers except the sled accelerometers and the sled velocity tachometer were referenced to the seat coordinate system. The sled accelerometers and the sled velocity tachometer were referenced to the sled coordinate system. The x-axis is horizontal and positive down track from the Horizontal Impulse Accelerator. The z-axis is vertical and positive upward. The y-axis is perpendicular to the x- and z-axes according to the right-hand rule.

Sled velocity was measured using a Globe Industries tachometer (Model 22A672-2). The rotor of the tachometer was attached to an aluminum wheel with a rubber "O" ring around its circumference to assure good rail contact. The wheel contacted the track rail and rotated as the sled moved, producing an output voltage proportional to the velocity.

### Load Cell Transducers

The specific load cells used are listed in the Instrumentation Tables at the end of this report. The tables also provide channel assignments and sensor sensitivities.

Shoulder and lap belt forces were measured using four GM 3D-SW load cells, each capable of measuring forces in the X, Y and Z directions. The lap anchor force triaxial load cells were located on separate brackets mounted on the side of the seat frame parallel to the seat pan (Figure A-7). The shoulder strap force triaxial load cell was mounted on the seat frame between the seat back support plate and the headrest (see Figure A-4 above).

Left, right and center seat pan forces were measured using three load cells and three load links (Figure A-8). Strainsert Model FL2.5U-2SPKT load cells were used to measure seat pan loads. The three load links used Micro Measurement Model EA-06-062TJ-350 strain gages. All measurement devices were located under the seat pan support plate. The load links were used for measuring loads in the x and y directions, two in the x direction and one in the y direction. Each load link housed a swivel ball, which acted as a coupler between the seat pan and load cell mounting plate (Figure A-10). The Strainsert load cells were used for measuring loads in the z direction.

Left, right and center seat back forces were measured using three load cells and three load links (Figure A-9). Strainsert Model FL2.5U-2SPKT load cells were used to measure seat pan loads. The three load links used Micro Measurement Model EA-06-062TJ-350 strain gages. All measurement devices were located behind the seat back support plate. The load links were used for measuring loads in the y and z directions, two in the y direction and one in the z direction. The Strainsert load cells were used for measuring loads in the x direction.

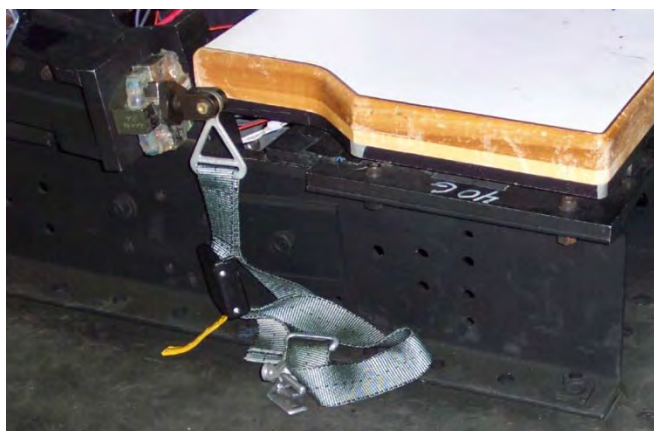


**Figure 7. Lap Belt Load Cell**



**Figure 8. Seat Pan Load Cells and Load Links**

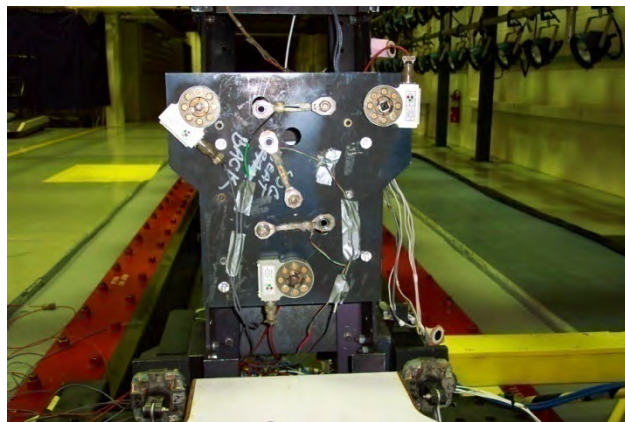


**Figure 9. Seat Back Load Cells and Load Links**

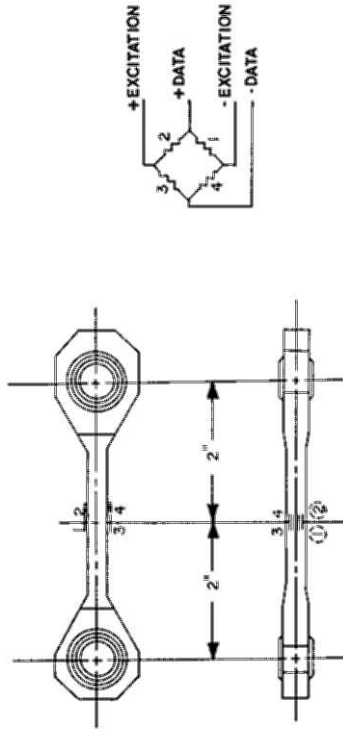


**Figure 10. Load Links**

### **Accelerometers**

A bite block fitted with three linear and one angular accelerometer measured human subject head accelerations. The chest accelerations were measured by an external package of linear x and angular y accelerometers secured to the chest using Velcro. For earplug subjects, a linear z accelerometer was affixed to the helmet or forehead. Internal accelerometer packages were mounted in the manikin chest and head. They were arranged to measure linear acceleration of the chest and head in all three axes and angular acceleration of the head about all three axes.

Sled x acceleration was measured using one Endevco Model 2262A-200 linear accelerometer. The accelerometer was mounted under the sled. Three Entran accelerometers were used to measure acceleration at the seat pan.

The specific accelerometers used are listed by type and impact axis in the Program Setup and Calibration Logs. The logs also provide individual sensor serial numbers, model numbers, channel assignments and sensor sensitivities.

### **Earplug Accelerometers**

The Delphi Earpiece Sensor System (DESS) was used for six of the earplug test human volunteer subjects. These custom-made earplug accelerometers were made individually for each subject for both left and right ears (Figure A-11). Inside each earplug were three accelerometers arranged to measure linear acceleration of the head in all three axes. The location measurements of the earplug accelerometers for each earplug subject are located in Table A-5.

**Table 5. Earplug Accelerometer Location Measurements**

		Subject ID					
		M-47	M-45	B-23	H-25	S-31	L-17
Location, Head Coordinate System (using Frankfort Plane)	Left Earplug X – Bite-bar Linear Accel X (Inches)	-5.02	-5.26	-5.67	-5.20	-5.90	-5.39
	Left Earplug Y – Bite-bar Linear Accel Y (Inches)	2.17	2.20	2.56	2.51	2.07	2.30
	Left Earplug Z – Bite-bar Linear Accel Z (Inches)	2.31	2.22	2.01	2.16	2.00	2.00
	Right Earplug X – Bite-bar Linear Accel X (Inches)	-5.02	-5.26	-5.67	-5.20	-5.90	-5.39
	Right Earplug Y – Bite-bar Linear Accel Y (Inches)	-3.77	-3.80	-4.16	-4.11	-3.67	-3.90
	Right Earplug Z – Bite-bar Linear Accel Z (Inches)	2.31	2.22	2.01	2.16	2.00	2.00
	Bite-bar angle wrt Frankfort plane (Degrees)	13.82	12.81	6.79	11.51	2.95	9.61
X-Axis Unit Vector, Head Coordinate System	Left X, Earplug Coordinate System	0.4876	0.7588	0.5249	0.8392	0.7372	0.7569
	Left Y, Earplug Coordinate System	0.3926	0.1768	0.3092	0.4520	0.3947	0.0494
	Left Z, Earplug Coordinate System	-0.7798	-0.6269	-0.7930	-0.3024	-0.5484	-0.6517
	Right X, Earplug Coordinate System	0.4876	0.7588	0.5249	0.8392	0.7372	0.7569
	Right Y, Earplug Coordinate System	-0.3926	-0.1768	-0.3092	-0.4520	-0.3947	-0.0494
	Right Z, Earplug Coordinate System	-0.7798	-0.6269	-0.7930	-0.3024	-0.5484	-0.6517
Y-Axis Unit Vector, Head Coordinate System	Left X, Earplug Coordinate System	-0.3516	-0.2740	-0.0986	-0.3188	-0.4309	-0.0856
	Left Y, Earplug Coordinate System	0.9059	0.9598	0.9475	0.8593	0.8998	0.9960
	Left Z, Earplug Coordinate System	0.2362	-0.0610	0.3042	0.4000	0.0683	-0.0240
	Right X, Earplug Coordinate System	0.3516	0.2740	0.0986	0.3188	0.4309	0.0856
	Right Y, Earplug Coordinate System	0.9059	0.9598	0.9475	0.8593	0.8998	0.9960
	Right Z, Earplug Coordinate System	-0.2362	0.0610	-0.3042	-0.4000	-0.0683	0.0240
Z-Axis Unit Vector, Head Coordinate System	Left X, Earplug Coordinate System	0.7991	0.5909	0.8454	0.4406	0.5204	0.6479
	Left Y, Earplug Coordinate System	0.1590	0.2181	-0.0815	-0.2393	0.1860	0.0739
	Left Z, Earplug Coordinate System	0.5798	0.7767	0.5278	0.8652	0.8334	0.7581
	Right X, Earplug Coordinate System	0.7991	0.5909	0.8454	0.4406	0.5204	0.6479
	Right Y, Earplug Coordinate System	-0.1590	-0.2181	0.0815	0.2393	-0.1860	-0.0739
	Right Z, Earplug Coordinate System	0.5798	0.7767	0.5278	0.8652	0.8334	0.7581



**Figure 11. Earplug Accelerometers**

### EMG Measurements

Electromyogram (EMG) measurements of the sternocleidomastoid and upper trapezius were recorded on ten subjects using a DelSys 8ch MyoMonitor (Figure A-12). Four electrodes and one reference electrode were utilized to measure the two muscles of interest of both sides of the neck. The MyoMonitor Data Logger is based on a modified Jornada 720 Handheld Computer made by Hewlett Packard. This unit was stored in a metal hinged box behind the headrest on the sled (Figure A-13).



Figure 12. DelSys MyoMonitor



Figure 13. EMG Storage Unit

### Transducer Calibration

Calibrations were performed before and after testing to confirm the accuracy and functional characteristics of the transducers. Pre-program and post-program calibrations are given in the Test Setup and Calibration Log. The Precision Measurement Equipment Laboratories (PMEL) at Wright-Patterson Air Force Base or General Dynamics personnel calibrated all Strainsert load cells.

The comparison method (Ensor, 1970) was used to calibrate the laboratory accelerometers. A laboratory standard accelerometer, calibrated on a yearly basis by Endevco with standards traceable to the National Bureau of Standards, and a test accelerometer were mounted on a shaker table. A random noise generator drove the shaker table and the accelerometer output was collected. The frequency response and phase shift of the test accelerometer were determined by using Fourier analysis on a PC. The natural frequency and the damping factor of the test accelerometer were determined, recorded and compared to previous calibration data for that test accelerometer.

Sensitivities were calculated at 20 G and 100 Hertz. The sensitivity of the test accelerometer was determined by comparing its output to the output of the standard accelerometer.

General Dynamics personnel calibrated the shoulder/lap triaxial load cells and load links. These transducers were calibrated to a laboratory standard load cell in a special test fixture. The sensitivity and linearity of each test load cell were obtained by comparing the output of the test load cell to the output of the laboratory standard under identical loading conditions. The laboratory standard load cell, in turn, is calibrated by PMEL on a regular basis.

The angular accelerometers are calibrated on a pre- and post-study basis by comparing their output to the output of a linear standard accelerometer. The angular sensors are mounted parallel to the axis of rotation of a Honeywell low inertia DC motor. The linear sensor is mounted perpendicular to the axis of rotation. An alternating current is supplied to the motor, which drives a constant sinusoidal angular acceleration of 100 Hz. The sensitivity of the angular accelerometer is calculated from the RMS output voltage to match the angular value computed from the linear standard.

The angular rate sensors are calibrated by comparing their output voltages to the acceleration difference between two linear standard accelerometers. The angular rate sensors are calibrated at 10 Hz.

General Dynamics personnel regularly calibrate the velocity wheel by rotating it at approximately 2000, 4000 and 6000 revolutions per minute (RPM) and recording both the output voltage and the RPM.

### **Data Acquisition**

The Sled Console Station controlled all data acquisition. Using a comparator, a test was initiated when the countdown clock reached zero. The comparator was set to start data collection at a pre-selected time. All data were collected at 1000 samples per second and filtered at a 120 Hz cutoff frequency using an 8-pole Butterworth filter.

Prior to placing a subject in the seat, data were recorded to establish a zero reference for all transducers. The reference data were stored separately from the test data and were used in the processing of the test data. A reference mark pulse was generated to mark the electronic data at a pre-selected time after test initiation to place the reference mark close to the impact point. The reference mark time was used as the start time for data processing of the electronic data.

### **EME DAS-64 Data Acquisition and Storage System**

The EME DAS-64 Data Acquisition and Storage System was used on the HIA for all tests (Figure A-14). It is a ruggedized signal conditioning and recording system for transducers and events. The system is powered by an external 19 volt DC power supply and communicates with the host computer through an RS-422 interface.

It is designed to withstand a 60 G, 100ms shock from a half sine shock profile in the three primary axes. It will also withstand 60 G amplitude, with a 10 to 2000 Hz sine sweep.

The EME DAS-64 will accommodate up to 64 transducer channels and 16 events. The signal conditioning front end excites, amplifies and offsets transducer input signals to appropriate levels for analog-to-digital conversion. Transducer signals are amplified, filtered, digitized and recorded

in the 4 Mbytes of onboard solid-state memory. The DAS was configured to collect data at 10K samples per second. At this sample rate it can hold 129,000 samples per channel. In post-processing, the sample files are decimated to 1K samples per second and filtered to cut off frequencies above 120 Hz.

The C program ADASEME on a desktop PC configured the DAS-64 prior to the start of the tests, transferred test data from the EME DAS-64 when the test was completed, and stored the collected test data in a binary data file. The program communicated with the EME DAS-64 Data Acquisition System by sending instructions over the RS-422 interface.



**Figure 14. EME DAS-64**

### **Delphi Accident Data Recorder 2**

The Delphi Accident Data Recorder 2 (ADR2) was used on the HIA for all earplug tests (Figure A-14). The ADR2 was used to record data from the six earplug accelerometers. It is a rugged recording system for transducers and events.

The ADR2 will accommodate up to 10 external signal inputs, comprised of 7 general purpose analog and 3 general purpose timer inputs. The parameters are recorded at 1,000 samples per second. The data are stored in ADR2 memory to be retrieved later via a high-speed data link to a PC.

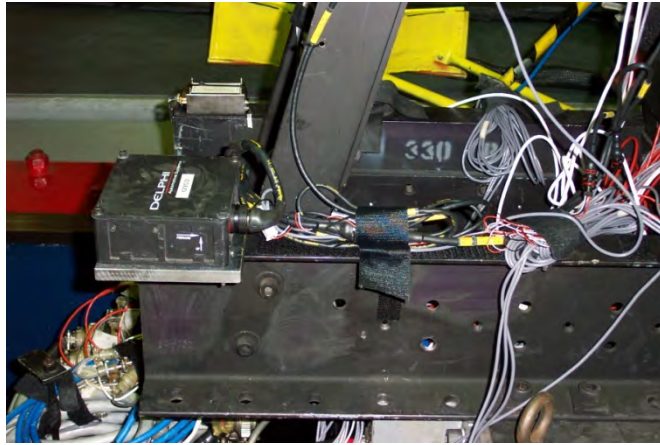


**Figure 15. Delphi ADR2**

### **Visual Fusion Motion Analysis Software**

Visual Fusion was designed to support analysis and understanding of target motion captured in a series of images. Analysis was performed on multiple image sequences obtained from two cameras (see Weinberger High Speed Video section) mounted on the HIA sled. The target motion included x, y, and z coordinates of each target versus time. Visual Fusion automatically tracks many targets in the field of view of the test section. The Visual Fusion target locations used in the VWHGX study are listed in Figure A-16.

The video is processed through Adobe Premier to allow for storage on the video hard drive and for processing by the Visual Fusion software. Motion analysis with Visual Fusion consists of three basic steps: processing, review, and analysis. In the processing step, targets are tracked and a history of target parameters (position, size, shape, intensity) is developed. During the review mode, the user clicks on targets in the imagery to select them for preliminary plots or to save as named targets for further detailed analysis. Finally, in the analysis step, the user can generate a number of sophisticated plots; import external data to plot along with Visual Fusion data; and perform 2-target analysis (e.g., separation distance), track editing, multi-sensor 3D position analysis or single-sensor 6-degree-of-freedom analysis. Results of the processing step are saved in an ASCII “track file” which contains all of the information about all targets tracked. Results of the review step are saved in individual “target files,” each of which contains the entire history of a single selected target.

The ‘Video3d’ program reads the Visual Fusion output files, filters the data, computes the velocity using an FIR filter, finds the extreme values, and converts the results into a format that is compatible with the AFRL Biodynamics Data Bank.

### Target ID and Location

1. Top of Head/Helmet top
2. Forehead/Helmet Forehead
3. Ear/Helmet Ear
4. Mouth
5. Chest
6. Shoulder
7. Front Bottom Frame
8. Back Bottom Frame
9. Mid Frame
10. Top Front Frame
11. Top Back Frame

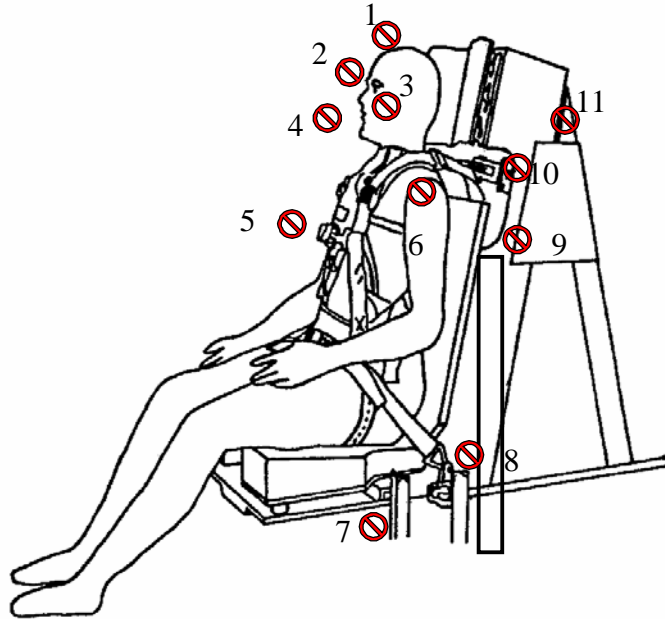


**Figure 16. Visual Fusion Target Locations**

### **Weinberger High-Speed Video**

Two carriage-mounted Weinberger SpeedCam Visario cameras (Figure A-17) were used to collect video and target motion data. One camera was mounted directly to the side of the sled, while the other was mounted at an oblique angle to the sled (Figure A-18). The camera location measurements are listed in Table A-6. The origin for the cameras that was used for the measurements was on the left side of the seat 198 mm in front of the back edge of the seat. The SpeedCam system is capable of data acquisition at up to 10,000 frames per second. The SpeedCam system is controlled via software specifically designed for Windows2000. The Control Unit allows for simultaneous operation of multiple cameras and controls the entire data management from system control, post-processing and visualization, to archiving of the completed image sequences.

The interface between cameras and the Control Unit occurs via LocalLinks. LocalLinks are system-specific cables 5 and 15 meters in length, which carry all video and control data as well as the power supply for the connected camera-heads.

The images for the VWHGX Study were collected at 500 frames/second. The video files were downloaded and converted to AVI format, and placed in the HEPA Biodynamics Data Bank.



**Figure 17. Weinberger SpeedCam Camera**

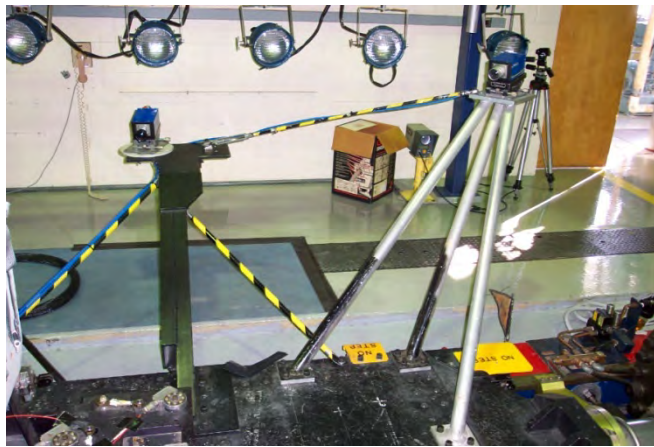


**Figure 18. Camera Locations**

**Table 6. Camera Location Measurements**

Video Measurements 16-Jan-03

Description	X (mm)	Y (mm)	Z (mm)
SRP	0.0	0.0	0.0
Top Front Frame	-197.1	204.2	704.6
Top Back Frame	-421.1	184.2	807.6
Mid Frame	-364.8	203.2	467.4
Bottom Frame	-67.9	280.0	12.5
Side Camera	298.4	1567.7	301.3
Oblique Camera	1761.1	1043.3	688.1

Video Measurements 26-Aug-03

Description	X (mm)	Y (mm)	Z (mm)
Top Front Frame	-195.1	174.7	741.3

**Data Processing**

The Excel 2000 Workbook VwhgxHac.xls is used to analyze the EME DAS test data from the VWHGX Study (HIA Facility). VwhgxHac.xls contains the Visual Basic module Module1 and the forms UserForm1 and UserForm2. Module1 contains one main subroutine that calls numerous other subroutines and functions. VwhgxHac.xls calls the DLL functions in the Dynamic Link

Libraries ScanDll1, Mathdll and FortranMathDll. The shortcut ctrl+r can be used to execute the Visual Basic module. The Visual Basic module displays the two user forms.

UserForm1 requests the user to enter the system acronym, study description, impact channel number, magnitude of the impact start level, start time, processing time, T0 bit number and reference mark bit number. The user has the option to find the Weinberger start time, start at the reference mark time, and use the processing time as the impact window time. The user has the option to plot the channels, print out the summary sheet, print out the plots, update the Access database information for the Biodynamics Data Bank, and create an Excel time history workbook for the Biodynamics Data Bank. Default values are displayed based on the last test that was analyzed. The default values are stored in worksheet "Defaults" inside the workbook.

UserForm2 requests the user to enter the test number for each test to be processed. The default test parameters are retrieved from the test sensitivity file and displayed on the form. The user may specify new values for any of the displayed test parameters. The test parameters include the subject ID, weight, age, height and sitting height. Additional parameters include the cell type, nominal g level, subject type (manikin or human), and belt pre-load status (computed or not computed), if used.

The workbook contains worksheets named "Channels," "Formulas," "Preloads," "Plots," "Time History File," "Plot Pages" and "Defaults." The "Channels" worksheet contains the channel number, channel name, database ID number, channel description, and summary sheet description for each channel. The "Formulas" worksheet contains Excel formulas and other data analysis functions. The "Preloads" worksheet contains the pre-load numbers and descriptions. The "Plots" worksheet contains the channel name, the plot description, and the plot vertical axis minimum, maximum and increment for each channel to be plotted. The "Time History File" worksheet defines the channel names for the time history files (the database time history files do not use this worksheet). The "Plot Pages" worksheet allows the user to print out selected plot pages (by default, all plot pages are printed). VwhgxHac.xls generates time histories for all channels, resultants, sums, and other calculated time histories.

Values for the pre-impact level and the extrema for each time history are stored in the Excel worksheet summary file and printed out as a summary sheet for each test. The time histories are also plotted with up to six plots per page. The user has the option to create test summary information and Excel workbooks containing the time histories for the Biodynamics Data Bank. VwhgxHac.xls automatically stores the test parameters, preloads and extrema values in an SQL Server database that contains the test data from ongoing test programs. This allows the test data to be viewed immediately following the test from an internal web site for ongoing test programs.

## **APPENDIX C: Subject Anthropometry Data**

### Subject Anthropometry Data

SUBJECT ID	GENDER	AGE (YR)	WEIGHT (LB)	STAND HT. (IN)	SITTING HT. (IN)
B-09	M	34	164	68.1	35.2
B-23	M	37	189	70.9	37.2
B-34	F	20	135	63.7	34.1
B-39	F	21	122	60.8	32.8
B-40	F	46	154	64.1	33.9
C-21	M	35	180	69.9	36.7
C-28	M	35	198	71.5	37.8
C-29	M	26	173	68.8	37.6
C-30	F	24	164	68.6	36.4
D-17	F	24	160	67.0	34.8
H-25	M	32	213	73.4	38.3
H-26	F	25	135	64.0	35.1
H-27	F	32	144	67.0	35.2
J-15	F	28	163	65.8	33.8
K-14	M	30	159	72.9	39.5
L-17	F	25	151	64.8	34.0
L-19	M	26	192	70.8	37.4
L-23	F	29	185	67.2	34.0
M-33	F	30	129	61.3	33.9
M-34	M	32	283	73.9	37.6
M-37	M	33	163	70.0	36.2
M-45	M	24	157	68.0	35.0
M-47	M	31	184	70.5	36.6
P-08	F	28	145	63.1	33.7
P-13	M	25	164	69.3	36.5
R-25	M	34	171	70.3	35.6
R-26	M	21	196	73.8	36.6
S-31	M	27	188	72.3	37.5
S-32	M	36	261	72.0	38.1
S-34	F	23	184	61.4	33.3
S-35	F	19	145	68.8	35.3
T-11	F	24	119	57.6	31.2
T-20	M	24	147	67.7	35.7
W-14	F	29	123	68.6	35.1
Mean		28.5	168.7	67.9	35.6
Std Dev		5.8	35.4	4.1	1.8

## **APPENDIX D: Electronic Data Channels**

**Table D-1: Electronic Data Channel List**

Channel No.	Parameter	Dynamic Range	Frequency Range
1	Sled X Accel	20 G	DC – 120 Hz
2	Sled Y Accel	20G	DC – 120 Hz
3	Sled Z Accel	10 G	DC – 120 Hz
4	Seat Pan X Accel	20 G	DC – 120 Hz
5	Seat Pan Y Accel	20 G	DC – 120 Hz
6	Seat Pan Z Accel	10 G	DC – 120 Hz
7	Head X Accel	50 G	DC – 120 Hz
8	Head Y Accel	20 G	DC – 120 Hz
9	Head Z Accel	30 G	DC – 120 Hz
10	Head Ry Ang. Accel	5000 Rad/Sec <sup>2</sup>	DC – 120 Hz
11	Chest X Accel	50 G	DC – 120 Hz
12	Chest Y Accel	20 G	DC – 120 Hz
13	Chest Z Accel	30 G	DC – 120 Hz
14	Chest Ry Ang. Accel	2000 Rad/Sec <sup>2</sup>	DC – 120 Hz
15	T1 X Accel	50 G	DC – 120 Hz
16	T1 Y Accel	20 G	DC – 120 Hz
17	T1 Z Accel	30G	DC – 120 Hz
18	Head Rest X Force	1000 lb	DC – 120 Hz
19	Head Rest Y Force	1000 lb	DC – 120 Hz
20	Head Rest Z Force	1000 lb	DC – 120 Hz
21	Left Shoulder X Force	1000 lb	DC – 120 Hz
22	Left Shoulder Y Force	1000 lb	DC – 120 Hz
23	Left Shoulder Z Force	1000 lb	DC – 120 Hz
24	Right Shoulder X Force	1000 lb	DC – 120 Hz
25	Right Shoulder Y Force	1000 lb	DC – 120 Hz
26	Right Shoulder Z Force	1000 lb	DC – 120 Hz
27	Left Lap X Force	1000 lb	DC – 120 Hz
28	Left Lap Y Force	1000 lb	DC – 120 Hz
29	Left Lap Z Force	1000 lb	DC – 120 Hz
30	Right Lap X Force	1000 lb	DC – 120 Hz
31	Right Lap Y Force	1000 lb	DC – 120 Hz
32	Right Lap Z Force	1000 lb	DC – 120 Hz
33	Left Seat Pan X Force	1000 lb	DC – 120 Hz
34	Right Seat Pan X Force	1000 lb	DC – 120 Hz
35	Seat Pan Y Force	1000 lb	DC – 120 Hz
36	Left Seat Pan Z Force	1000 lb	DC – 120 Hz
37	Right Seat Pan Z Force	1000 lb	DC – 120 Hz
38	Center Seat Pan Z Force	1000 lb	DC – 120 Hz

**Table D-2: Additional Electronic Data Channels: ADAM Tests**

Channel No.	Parameter	Dynamic Range	Frequency Range
39	Int Head X Accel	50 G	DC – 120 Hz
40	Int Head Y Accel	20 G	DC – 120 Hz
41	Int Head Z Accel	30 G	DC – 120 Hz
42	Int Head Rx Ang. Accel	5000 Rad/Sec <sup>2</sup>	DC – 120 Hz
43	Int Head Ry Ang Accel	5000 Rad/Sec <sup>2</sup>	DC – 120 Hz
44	Int Head Rz Ang. Accel	5000 Rad/Sec <sup>2</sup>	DC – 120 Hz
45	Int Chest X Accel	50 G	DC – 120 Hz
46	Int Chest Y Accel	20 G	DC – 120 Hz
47	Int Chest Z Accel	30 G	DC – 120 Hz
48	Int Chest Ry Ang Accel	5000 Rad/Sec <sup>2</sup>	DC – 120 Hz
49	Int Neck X Force	1000 lb	DC – 120 Hz
50	Int Neck Y Force	500 lb	DC – 120 Hz
51	Int Neck Z Force	500 lb	DC – 120 Hz
52	Int Neck Mx Torque	500 in-lb	DC – 120 Hz
53	Int Neck My Torque	1000 in-lb	DC – 120 Hz
54	Int Neck Mz Torque	500 in-lb	DC – 120 Hz
55	Sled Velocity	100 Ft/Sec	DC – 120 Hz
D-3	Reference		Digital Input
D-4	T = 0 Pulse		Digital Input

## **APPENDIX E: Weight and Center-of-Gravity of Helmet Configurations**

### Summary of VWI Helmet Configurations

Nominal Helmet Weight (lbs)	Helmet Size and Configuration Description	Actual Helmet Weight (lbs)	CGX (in)	CGY (in)	CGZ (in)
2.0	Medium HGU-55/P, Thermal Plastic Liner, no mask, no visor, non-ICNS	2.0	-1.24	-0.03	1.73
	Large HGU-55/P, Thermal Plastic Liner, no mask, no visor, non-ICNS	2.1	-1.2	0.02	1.43
	X-Large HGU-55/P, Thermal Plastic Liner, no mask, no visor, non-ICNS	2.2	-0.92	0.08	1.09
3.0	Medium HGU-55/P VIP, Zeta Liner, MBU-12/P Mask cut away, halo 3rd hole from extreme forward	2.8	-0.16	0.02	1.74
	Large HGU-55/P VIP, Zeta Liner, MBU-12/P Mask cut away, no weights	2.91	0.11	0.02	1.17
	X-Large HGU-55/P VIP, TPL, MBU-12/P Mask cut away, Std ear cups, no laser, no weights	2.98	0.32	0.23	1
3.5	Medium HGU-55/P VIP, TPL, 0.5 Lbs (0.25x2) 4.5" from extreme aft, MBU-12/P Mask cut away, Std ear cups	3.31	0.19	0.01	1.72
	Large HGU-55/P VIP, Zeta Liner, 0.5 Lbs (0.25x2) 6.5" from center post, MBU-12/P Mask cut away, Std Ear cups	3.42	0.47	0.02	1.17
	X-Large HGU-55/P VIP, TPL, 0.5 Lbs (0.25x2) 6.5" from center post, MBU-12/P Mask cut away (long), Std ear cups	3.48	0.64	0.25	1.03
4.0	Medium HGU-55/P VIP, Zeta Liner, 1.0 Lbs (0.5x2) 1.5" from center post, MBU-20/P Mask cut away, Std ear cups	3.81	1.51	0.03	1.95
	Large HGU-55/P VIP, Zeta Liner, 1.0 Lbs (0.5x2) 1.25" from center post, MBU-12/P Mask cut away, Std ear cups	3.9	1.71	-0.03	1.52
	X-Large HGU-55/P VIP, TPL, 1.0 Lbs (0.5x2) 1.25" from center post, std ear cups MBU-12/P Mask cut away (Long)	3.99	1.93	0.3	1.44
4.5	Medium HGU-55/P VIP, Zeta Liner, 1.5 Lbs (0.75x2) 3.5" from center post, MBU-20/P Mask cut away	4.3	1.8	0.06	1.96
	Large HGU-55/P VIP, Zeta Liner, 1.5 Lbs (0.75x2) 3.5" from center post, MBU-12/P Mask cut away, Std ear cups	4.41	1.99	-0.04	1.53
	X-Large HGU-55/P VIP, TPL, 1.5 Lbs (0.75x2) 3.5" from center post, std ear cups, MBU-12/P Mask cut away (long)	4.48	2.18	0.28	1.47

## **APPENDIX F: Neck Load Program**

## NeckLoad4

An in-house software program, “Neckload4”, was designed to calculate neck forces and moments using measured head linear and angular accelerations and inertial properties of the helmet, head, and neck. The program calculates the force and moment at the occipital condyles (OC or head-neck junction). An additional sub-routine in this program described in a previous report by Gallagher<sup>5</sup> also allows the user to calculate the force and moment at the C1/C2 junction, C4/C5 junction, and/or C7/T1 junction. These calculated forces and moments experienced by the human head and neck (Figure F-1) are based on the equations of motion for rigid bodies or systems. This program separates the head, neck, and helmet into two systems: the head and neck are combined as the first system and the helmet is the second system.

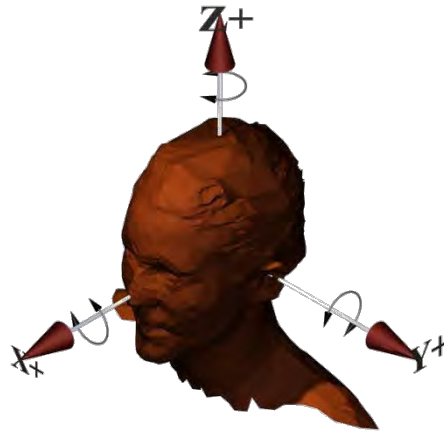


**Figure F-1: Anatomical Axis System of the Human Head and Neck.**

### Head Mass/Center of Mass.

The following regression equation is used to determine the subject’s head mass. Clauser, et al.<sup>4</sup> predicted the head mass in kilograms by using the subject’s measured head circumference and body weight.

$$\text{Head Mass} = 0.104 * \text{Head Circumference} + 0.015 * \text{Body Weight} - 2.189$$

The center of mass of the head is assumed to be at the average location for the head center of gravity determined by Beier.<sup>2</sup> The mean and standard deviation for the head center of gravity were calculated from twenty-one fresh cadavers. The three-dimensional location of the center of gravity of the head was related to the anatomically based coordinate reference system (Table F-1).

**Table F-1: Head Center of Gravity<sup>2</sup>**

Coordinates of Head Center of Gravity	Mean and Standard Deviation (cm)
X	0.83 +/- 0.25
Y	-0.05 +/- 0.13
Z	3.12 +/- 0.56

Total Neck Supported Mass/Center of Mass.

Biodynamic response data are collected by an on-board data acquisition system during testing on the Horizontal Impulse Accelerator (HIA) at Wright-Patterson AFB, Ohio. The subject is instrumented with accelerometers. Head linear and angular accelerations are measured with a tri-axial accelerometer and an angular accelerometer array mounted on a bite bar. The head acceleration is normalized to eliminate the variations in carriage acceleration.

The inertial properties of the helmet were previously measured by General Dynamics using the methods described in a report by Albery, et al.<sup>1</sup> and within the accuracies of the Standard Automated Mass Properties Measurement System as reported by Self, et al.<sup>6</sup>

Force and Moment Calculation.

The bite bar acceleration and the bite bar angular acceleration are used to compute the acceleration at the center of mass of the combined helmet, head and neck system. A 1G vector in the vertical direction was added to the measured bite bar acceleration when the head is in its initial position. As the bite bar accelerometer rotated, the bite bar acceleration always contained 1G in the vertical direction due to the force of gravity. The 1G vector is carried over to the computed acceleration at the center of mass. The 1G vector represents the weight of the combined system in the calculation. The force is computed based on the total mass and the acceleration at the center of mass. The torque is calculated based on the total mass, inertial tensor, acceleration at the center of mass, position relative to the center of mass, angular acceleration, and angular velocity.

The acceleration at the center of mass is:  $\vec{a}_{cm} = \vec{a} + \dot{\vec{\omega}} \times \vec{r} + \vec{\omega} \times (\vec{\omega} \times \vec{r})$ <sup>8</sup>, where  $a$  is the actual acceleration at the bite bar,  $\omega$  is the angular velocity,  $\dot{\omega}$  is the angular acceleration, and  $r$  is a vector from the bite bar accelerometer location to the center of mass. The angular velocity can be calculated by integrating the angular acceleration. However, the piezoresistive accelerometers measure a combination of the actual acceleration and the force of gravity:  $\vec{a} = \vec{a}_M - \vec{g}_0 + \vec{g}$ , where  $a_M$  is the measured acceleration at the bite bar as measured by the piezoresistive accelerometers,  $a$  is the actual acceleration at the bite bar and  $g_0$  is the initial acceleration of gravity vector at the time before the impact when the accelerometer is zeroed. The input bite bar acceleration that is read in by the Neckload4 program is assumed to be  $\vec{a}_M - \vec{g}_0$ , a value that is normally stored in the Biodynamic Data Bank.<sup>3</sup> Combining the two equations gives  $\vec{a}_{cm} - \vec{g} = \vec{a}_M - \vec{g}_0 + \dot{\vec{\omega}} \times \vec{r} + \vec{\omega} \times (\vec{\omega} \times \vec{r})$ .

### Force Calculation.

The force is then calculated using  $\vec{F} = m(\vec{a}_{cm} - \vec{g})$ ; where  $F$  is the force,  $m$  is the total mass of the combined helmet and head,  $a_{cm}$  is the acceleration at the center of mass, and  $g$  is a vector in the direction of the acceleration of gravity.

### Moment Calculation.

The moment (or torque) is calculated using:  $\vec{\tau} = \vec{R} \times m(\vec{a}_{cm} - \vec{g}) + I \cdot \dot{\vec{\omega}} + \vec{\omega} \times (I \cdot \vec{\omega})$ <sup>7</sup>, where  $\tau$  is the torque,  $R$  is a vector from the point at which the torque is calculated to the center of mass and  $I$  is the inertial tensor for the moments of inertia in the head anatomical coordinate system.<sup>8</sup> The torque represents the torque as it would be measured at the corresponding location in the neck.

The total mass and the location of the center of mass of the combined helmet and head system are calculated based on the masses and center of masses of the helmet and head. The inertial tensor of the combined system is calculated from the principal moments of inertia of the helmet and head by finding the inertial tensors of the individual components using:  $I = A I_p A^T$  where  $A$  is the direction cosine matrix,  $I$  is the inertial tensor in the anatomical coordinate system and  $I_p$  is the inertial tensor in the principle axis coordinate system. The inertial tensors of the individual components are then combined using the parallel-axis theorem.

Time histories and summary information about the calculated neck forces and moments are output and stored in an Excel workbook. The sign conventions use SAE J211 sign convention for the output which has the z-axis positive downward.

A source of error for the program is the use of regression equations. These equations do take into account some of the subject's true measurements, but the segment weights and inertial properties are still estimations. Also, the program calculates the acceleration at the center of mass based on the measured head linear and angular accelerations. Unfortunately, the angular accelerations are often noisy. The program gives the user the option to filter the angular acceleration, but the noise on the angular acceleration could cause the calculated acceleration at the center of mass to be higher than it should be.

A limitation of the Neckload4 program is that the program assumes that the linear and angular accelerations of the head are caused entirely by the neck forces. The forces due to the neck were assumed to be the only external force acting on the system. If external forces other than the neck (such as due to a headrest) were acting on the head, they would need to be subtracted out of the total force that is calculated by the program in order to find the neck force and moment. Consequently, the results from the program only accurately represent the neck force and moment for each axis direction during the time period when no other external forces are acting on the head in that direction.

## REFERENCES (for Appendix F)

- 1) Albery, C.B., Kaleps, I. (1997) A Procedure to Measure the Mass Properties of Helmet Systems. NDIA Design and Integration of Helmet Systems Symposium Proceedings. Framingham, MA.
- 2) Beier, G., Schuller, E., Schuck, M., Ewing, C.L., Becker, E.D., Thomas, D.J. (1980) Center of Gravity and Moments of Inertia of Human Heads. Scientific Report No. 1:218-228. Institute for Forensic Medicine, University of Munich. Naval Biodynamics Laboratory, New Orleans, LA.
- 3) Buhrman, J.R., Plaga, J.A., Cheng, H., Mosher, S.E. (2001) The AFRL Biodynamics Data Bank on the Web: A Repository of Human Impact Acceleration Response Data. Proceedings of the 39<sup>th</sup> Annual SAFE Symposium.
- 4) Clauser, C.E., McConville, J.T., Young, J.W. (1969) Weight, Volume, and Center of Mass of Segments of the Human Body. AMRL-TR-69-70.
- 5) Gallagher H.L., Buhrman J.R., Perry C.E., Mosher S.E., and Wilson D.D. (2007). An Analysis of Vertebral Stress and BMD During +Gz Accelerations. Air Force Technical Report AFRL-HE-WP-TR-2007-0085.
- 6) Self, B.P., Spittle, E.K., Kaleps, I., Albery, C.B. (1992) Accuracy and Repeatability of the Standard Automated Mass Properties Measurement System. AL-TR-1992-0137.
- 7) Symon, K.R. (1960) Mechanics, Addison-Wesley, p. 451.
- 8) Wells, D.A., (1967) Lagrangian Dynamics, Schaum's Outline Series, McGraw-Hill, p. 180.

## **APPENDIX G: Sample Acceleration/Force Data**

VWHGX Study Test: 7521 Test Date: 031209 Subj: J-15 Wt: 160.0  
 Nom G: 10.0 Cell: F

Data ID	Immediate Preimpact	Maximum Value	Minimum Value	Time Of Maximum	Time Of Minimum
Reference Mark Time (Ms)				-152.0	
Impact Rise Time (Ms)				68.0	
Impact Duration (Ms)				161.0	
Velocity Change (Ft/Sec)		33.14			
SLED X ACCEL (G)	0.00	9.93	-0.22	68.0	163.0
SLED Y ACCEL (G)	0.00	0.73	-0.57	56.0	63.0
SLED Z ACCEL (G)	1.00	2.44	0.54	16.0	28.0
SLED VELOCITY (FT/SEC)	0.12	32.61	0.16	171.0	0.0
INTEGRATED ACCEL (FT/SEC)	0.00	33.14	0.02	308.0	0.0
SEAT PAN X ACCEL (G)	0.00	0.87	-9.79	162.0	67.0
SEAT PAN Y ACCEL (G)	0.00	1.49	-1.44	75.0	123.0
SEAT PAN Z ACCEL (G)	0.99	2.94	0.46	59.0	16.0
HEAD X ACCEL (G)	0.00	4.68	-19.31	213.0	208.0
HEAD Y ACCEL (G)	0.02	1.49	-1.21	80.0	186.0
HEAD Z ACCEL (G)	1.01	7.46	-4.34	188.0	85.0
HEAD RESULTANT (G)	1.01	19.49	0.10	208.0	304.0
HEAD HIC		14.51		81.0	96.0
HEAD Ry ANG ACCEL (RAD/SEC2)	-1.36	525.68	-523.90	59.0	165.0
STERNUM X ACCEL (G)	0.22	6.97	-14.56	156.0	147.0
STERNUM Ry ANG VEL (RAD/SEC)	-0.02	32.10	-13.91	153.0	60.0
HEADREST X FORCE (LB)	22.58	31.44	-131.63	206.0	59.0
HEADREST X MINUS TARE (LB)	22.60	32.28	-82.65	206.0	59.0
HEADREST Y FORCE (LB)	-17.11	21.83	-58.25	85.0	64.0
HEADREST Z FORCE (LB)	6.38	62.64	-52.58	76.0	69.0
LEFT SHOULDER X FORCE (LB)	-81.16	-16.12	-342.88	205.0	78.0
LEFT SHOULDER Y FORCE (LB)	-10.84	1.86	-65.53	210.0	83.0
LEFT SHOULDER Z FORCE (LB)	11.26	104.29	-8.98	96.0	208.0
LEFT SHOULDER RESULTANT (G)	82.68	362.97	16.14	78.0	205.0
RIGHT SHOULDER X FORCE (LB)	-61.89	-14.79	-359.01	206.0	79.0
RIGHT SHOULDER Y FORCE (LB)	4.57	33.30	-2.83	92.0	201.0
RIGHT SHOULDER Z FORCE (LB)	27.55	95.32	17.19	95.0	198.0
RIGHT SHOULDER RES (LB)	68.16	371.23	22.70	79.0	207.0

Data ID	Immediate Preimpact	Maximum Value	Minimum Value	Time Of Maximum	Time Of Minimum
LEFT LAP X FORCE (LB)	-35.17	0.00	-700.40	217.0	92.0
LEFT LAP Y FORCE (LB)	14.84	139.65	-12.70	88.0	244.0
LEFT LAP Z FORCE (LB)	-59.18	-5.71	-512.57	223.0	92.0
LEFT LAP RESULTANT (LB)	70.62	878.78	10.85	93.0	225.0
RIGHT LAP X FORCE (LB)	-40.05	-4.39	-768.96	225.0	90.0
RIGHT LAP Y FORCE (LB)	-9.81	7.52	-144.34	209.0	96.0
RIGHT LAP Z FORCE (LB)	-56.40	-4.39	-451.21	217.0	91.0
RIGHT LAP RESULTANT (LB)	70.07	902.41	7.96	91.0	227.0
LEFT SEAT PAN X FORCE (LB)	46.70	114.64	-47.46	233.0	84.0
RIGHT SEAT PAN X FORCE (LB)	59.89	93.91	-81.81	232.0	87.0
SEAT PAN X SUM (LB)	106.59	207.57	-126.33	233.0	85.0
SEAT PAN X MINUS TARE (LB)	106.71	210.94	11.39	232.0	344.0
SEAT PAN Y FORCE (LB)	14.96	138.21	-11.18	96.0	343.0
LEFT SEAT PAN Z FORCE (LB)	-11.83	231.00	-16.12	94.0	1.0
RIGHT SEAT PAN Z FORCE (LB)	13.29	261.60	-13.87	92.0	296.0
CENTER SEAT PAN Z FORCE (LB)	283.01	721.91	120.24	90.0	283.0
SEAT PAN Z SUM (LB)	284.47	1207.67	103.92	91.0	283.0
SEAT PAN RESULTANT (LB)	304.17	1220.30	107.87	91.0	283.0
SEAT PAN RES MINUS TARE (LB)	304.21	1220.54	107.77	91.0	283.0
LEFT SEAT BACK X FORCE (LB)	15.29	199.98	-15.38	209.0	217.0
RIGHT SEAT BACK X FORCE (LB)	28.20	249.23	-32.95	201.0	206.0
SEAT BACK X FORCE (LB)	77.36	263.76	-46.83	213.0	219.0
SEAT BACK X SUM (LB)	120.85	419.53	-19.97	235.0	15.0
SEAT BACK X MINUS TARE (LB)	120.99	422.58	-15.21	235.0	162.0
TOP SEAT BACK Y FORCE (LB)	2.24	147.17	-143.36	48.0	69.0
BOT SEAT BACK Y FORCE (LB)	20.12	80.28	-157.04	69.0	64.0
SEAT BACK Y SUM (LB)	22.36	126.86	-65.52	88.0	68.0
SEAT BACK Z FORCE (LB)	8.65	137.36	-210.32	60.0	67.0
SEAT BACK RESULTANT (LB)	123.21	423.69	4.01	235.0	165.0
SEAT BACK RES MINUS TARE (LB)	123.35	426.71	2.83	235.0	186.0

VWHGX Study Test: 7521 Test Date: 031209 Subj: J-15 Wt: 160.0  
 Nom G: 10.0 Cell: F

Data ID	Immediate Preimpact	Maximum Value	Minimum Value	Time Of Maximum	Time Of Minimum
LEFT FOOT X FORCE (LB)	20.68	29.10	-341.93	138.0	63.0
LEFT FOOT Y FORCE (LB)	2.13	45.99	-2.83	62.0	72.0
LEFT FOOT Z FORCE (LB)	-16.22	5.57	-156.55	262.0	68.0
LEFT FOOT RESULTANT (LB)	26.70	373.36	8.12	64.0	287.0
CORR LEFT FOOT X FORCE (LB)	3.16	12.77	-345.57	246.0	64.0
CORR LEFT FOOT Z FORCE (LB)	-26.09	143.52	-54.62	63.0	129.0
RIGHT FOOT X FORCE (LB)	13.41	19.23	-294.18	372.0	61.0
RIGHT FOOT Y FORCE (LB)	12.23	29.40	-25.30	10.0	148.0
RIGHT FOOT Z FORCE (LB)	-7.42	24.32	-145.61	247.0	67.0
RIGHT FOOT RESULTANT (LB)	20.10	314.98	1.98	61.0	167.0
CORR RIGHT FOOT X FORCE (LB)	4.24	23.20	-287.50	247.0	61.0
CORR RIGHT FOOT Z FORCE (LB)	-26.09	143.52	-54.62	63.0	129.0

